Universidade de Aveiro
2012
Departamento de Secção Autónoma de Ciências da Saúde

BRUNO FILIPE PIMPAREL GONÇALVES

Digital Imaging Processing Tools for Neuronal Images

Ferramentas de Processamento Digital de Imagem para Imagens Neuronais

Universidade de Aveiro
2012
Departamento de Secção Autónoma de Ciências da Saúde

BRUNO FILIPE PIMPAREL GONÇALVES

Digital Imaging Processing Tools for Neuronal Images

Ferramentas de Processamento Digital de Imagem para Imagens Neuronais

Dissertação apresentada à Universidade de Aveiro para cumprimento dos requisitos necessários à obtenção do grau de Mestre em Biomedicina Molecular, realizada sob a orientação científica do Professor Doutor Augusto Marques Ferreira da Silva, Professor Auxiliar do Instituto de Engenharia Electrónica e Telemática da Universidade de Aveiro e da Professora Doutora Sandra Isabel Moreira Pinto Vieira, Professora Auxiliar Convidada da Secção Autónoma de Ciências da Saúde da Universidade de Aveiro.

Este trabalho contou com o apoio do Centro de Biologia Celular (CBC) da Universidade de Aveiro, e é financiado por fundos FEDER através do Programa Operacional Factores de Competitividade – COMPETE e por Fundos nacionais da FCT – Fundação para a Ciência e a Tecnologia no âmbito dos projectos PTDC/QUI-BIQ/101317/2008, PTDC/SAL-NMC/111980/2009 e PEst-OE/SAU/UI0482/2011.

Dedico à minha família que sempre me apoiou.

o júri

presidente

Professora Doutora Odete Abreu Beirão da Cruz e Silva
Prof. Auxiliar com Agregação, Secção Autónoma de Ciências da Saúde, Universidade de Aveiro

Professor Doutor Augusto Marques Ferreira da Silva
Prof. Auxiliar no Departamento de Eletrónica e Telecomunicações e Informática da Universidade de Aveiro

Professora Doutora Sandra Isabel Moreira Pinto Vieira
Prof. Auxiliar Convidada da Secção Autónoma da Saúde da Universidade de Aveiro

Doutora Daniela Maria Oliveira Gandra Ribeiro
Investigadora do Centro de Biologia Celular, Universidade de Aveiro

agradecimentos

Ao meu orientador Augusto Silva por todo o apoio e dedicação durante a elaboração deste trabalho.

À minha coorientadora Sandra Vieira por toda a dedicação e ajuda que me deu não só durante a elaboração deste trabalho mas durante todo o meu percurso como estudante universitário.

À professora Odete da Cruz e Silva, pela oportunidade de realizar este trabalho no laboratório de Neurociências do Centro de Biologia Celular.

À minha família, pelo seu incentivo e apoio contínuo que sempre me deram.

Ao Igor Marques e Roberto Dias pela ajuda que me deram na revisão deste trabalho.

A todos os meus colegas do CBC, em especial à Regina Cerqueira e à Joana Rocha.

A todos os meus amigos de Ciências Biomédicas, em especial à Maria João, à Joana Tavares, ao Roberto Dias, ao Rui João, ao Igor Marques, à Carina Bernardo, à Liliana Oliveira e à Catarina Coelho, pelos momentos de lazer e descontração que foram fundamentais para vencer o cansaço.

À FCT pelo financiamento dos projetos PTDC/QUI-BIQ/101317/2008 e PTDC/SAL-NMC/111980/2009.

palavras-chave

Análise de imagem; morfologia neuronal; imagens de microscopia de fluorescência e contraste de fase; ImageJ; NeuronJ; NeuriteQuant; NeurphologyJ; NeuroNet.

resumo

Os neurónios são celulas especializadas do Sistema Nervoso, cujas funções se baseiam na correta formação de três compartimentos subcelulares primários – corpo celular, axónio e dendrites – e na rede neuronal que formam para passar a informação entre si.

A análise quantitativa das características destas estruturas pode ser usada para estudar a relação entre a morfologia e função neuronal, e monitorizar alterações que ocorram em células individuais ou ao nível da rede, que se possam correlacionar com doenças neurológicas.

Nesta tese foi efetuada uma pesquisa de ferramentas digitais disponíveis dedicadas ao processamento e análise de imagens neuronais, com enfoque na sua aplicabilidade para analisar as nossas bioimagens neuronais de fluorescência adquiridas no dia-a-dia. Nos programas selecionados (NeuronJ, NeurphologyJ e NeuriteQuant) foi primeiro avaliada a necessidade de pre-processamento, e os programas foram subsequentemente utilizados em conjuntos de imagens de culturas primárias de córtex de rato para comparar a sua eficácia no processamento destas bioimagens. Os dados obtidos com os vários programas foram comparados com a análise manual usando o ImageJ como ferramenta de análise.

Os resultados demonstraram que o programa que aparenta funcionar melhor com as nossas imagens de fluorescência é o NeuriteQuant, porque é automático e dá resultados globalmente semelhantes aos da análise manual, especialmente na avaliação do Comprimento das Neurites por célula. Uma das desvantagens é que a quantificação da ramificação das neurites não dá resultados satisfatórios e deve continuar a ser realizada manualmente.

Também realizamos uma pesquisa de ferramentas de processamento de imagem dedicada a imagens de contraste de fase, mas poucos programas foram encontrados. Estas imagens são mais fáceis de obter e mais acessíveis economicamente, contudo são mais difíceis de analisar devido às suas características intrínsecas.

Para contornar esta lacuna, estabeleceu-se e otimizou-se uma sequência de processamento e análise para melhor extrair informação neuronal relevante de imagens de contraste de fase utilizando o programa ImageJ.

A sequência desenvolvida, na forma de uma macro do ImageJ designada NeuroNet, foi aplicada a imagens de contraste de fase de culturas neuronais em diferentes dias de diferenciação, na presença ou ausência de um inibidor farmacológico, com o objetivo de responder a uma questão científica.

A macro NeuroNet desenvolvida provou ser útil para analisar estas bioimagens, existindo contudo espaço para ser aperfeiçoada.

keywords

Image analysis; neuron morphology; fluorescence and phase contrast microscopy; ImageJ; NeuronJ; NeurphologyJ; NeuriteQuant; NeuroNet

abstract

Neurons are specialized cells of the Nervous System, with their function being based on the formation of the three primary sub cellular compartments – soma, axons, and dendrites – and on the neuritic network they form to contact and pass information to each other.
The quantitative analysis of the characteristics of these structures can be used to study the relation between neuronal morphology and function, and to monitor distortions occurring in individual cells or at the network level that may correlate with neurological diseases.
In this thesis a survey of freely available digital tools dedicated to neuronal images processing and analysis was made with an interest in their applicability to analyse our routinely acquired neuronal fluorescent bioimages. The selected program´ (NeuronJ, NeurphologyJ and NeuriteQuant) preprocessing requirements were first evaluated, and the programs were subsequently applied to a set of images of rat cortical neuronal primary cultures in order to compare their effectiveness in bioimage processing. Data obtained with the various programs was compared to the manual analysis of the images using the ImageJ analysis tool.
The result show that the program that seems to work better with our fluorescence images is NeuriteQuant, since it is automatic and gives overall results more similar to the manual analysis. This is particularly true for the evaluation of the Neurite Length per Cell. One of the drawbacks is that the quantification of neuritic ramification does not give satisfactory results and is better to be performed manually.
We also performed a survey of digital image processing tools dedicated to phase contrast microphotographs, but very few programs were found. These images are easier to obtain and more affordable in economic terms, however they are harder to analyse due to their intrinsic characteristics.
To surpass this gap we have established and optimized a sequence of steps to better extract relevant information of neuronal phase contrast images using ImageJ.
The work-flow developed, in the form of an ImageJ macro named NeuroNet, was then used to answer a scientific question by applying it to phase contrast images of neuronal cultures at different differentiating days, in the presence or absence of a pharmacological inhibitor.
The developed macro NeuroNet proved to be useful to analyse the images however there is still space to improvement.

Contents

List of Figures

List of Tables

List of Acronyms

APP Amyloid Precursor Protein

CBC Neuroscience Laboratory

CLAHE Contrast Limited Adaptive Histogram Equalization

CNS central nervous system

div days in vitro

DAPT N-[N-(3,5- difluorophenacetyl)-l-alanyl]-S-phenylglycine t-butyl ester

DoG Difference of Gaussians

GPP green fluorescent protein

MAP2 Microtubule-associated protein 2

PNS peripheral nervous system

SNAP-25 Synaptosomal-associated protein 25

Chapter 1

Introduction

1.1 Neuronal imaging

This thesis focuses on the characterization and comparison of freely available processing tools for the analysis of neuronal bioimages. These are images recorded from biological samples, mainly through the use of microscopes, and are named 'bio' in contrast to images of neurons and neural networks digitally created.

The neuronal bioimages are difficult to analyse, mainly due to their biological nature. Neurons develop a complex neuritic network and therefore neuronal cultures can present huge variations of morphology and intensity from image to image. Problems such as low contrast and uneven illumination are relatively common and, besides deriving from imaging technical limitations, they also derive from unevenly distributed neuronal populations, out of focus neurites, typical shorter dimensions of neuronal cells (in terms of height), resulting in lower phase contrast[1].

For example Figure 1.1 and 1.2 are images from fluorescence and phase contrast microscopy, respectively, and represent typical images routinely acquired in the Neuroscience Laboratory (CBC). It is possible to see in Figure 1.1 that the quality of the image is low due to low contrast and low signal to noise ratio, as thick and thin and bright and dim neurites coexist in the same image. Figure 1.2 is further complicated by a poorly differentiated background (very low signal to noise ratio), in which the neurites appear discontinuous along their paths, the cell body and neurites can be out of focus, and various dead cells can be observed that may be considered as false positives.

Neuronal bioimage processing has evolved since its beginning four decades ago, when processing was made by elementary manual interaction with computer recorded images obtained through standard light microscopy. Nowadays, despite several academic and commercially available tools, neuroanatomists still struggle with the lack of generalized applicability of the available tools, and the vast majority of axons and dendrites are still traced manually [2] [3].

This thesis will present some techniques and tools that have been successfully used in quantitative image analysis tasks and thus provide a relevant contribution towards neu-

ronal morphology assessment. The major goal is to develop successful work-flows for the quantitative analysis of fluorescence and phase contrast photomicrographs obtained in the CBC.

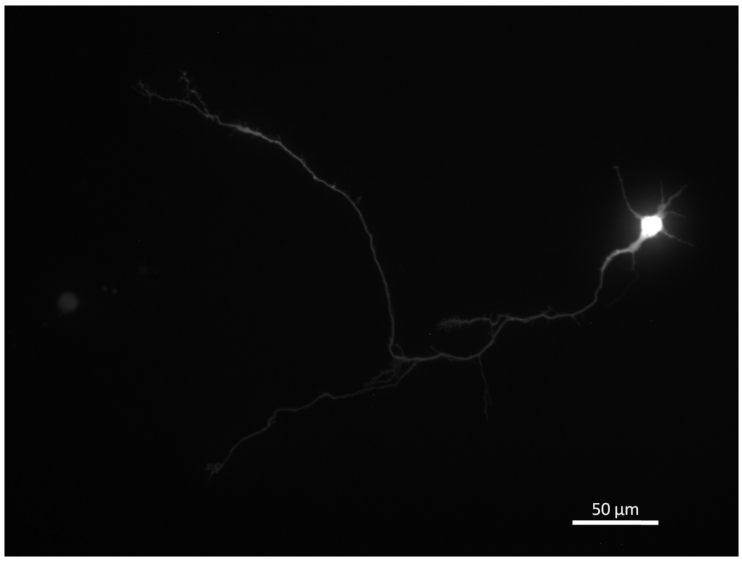

Figure 1.1: Routine fluorescence microscopy bioimage of a single neuron expressing the fluorescent protein GPF in a non-fluorescent background, in a cortical primary neuronal 2D culture at 4 div.

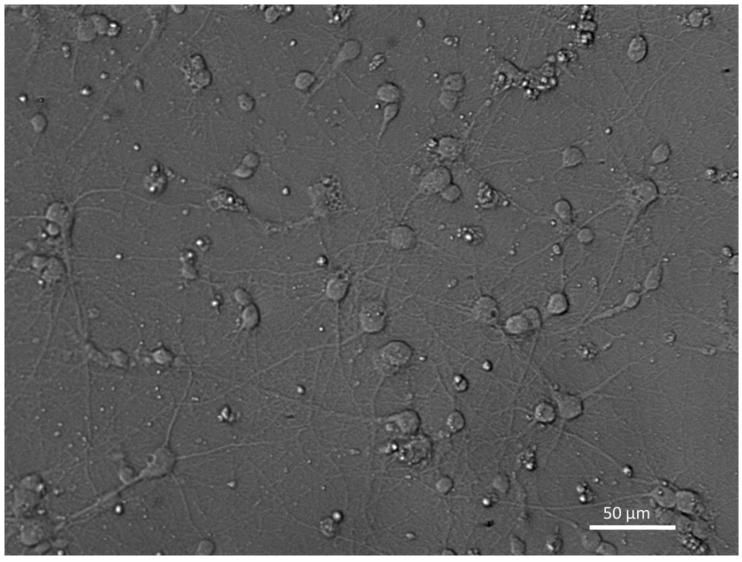

Figure 1.2: Typical phase contrast microscopy bioimage of a primary neuronal 2D culture (10 days in vitro).

1.2 Neuronal morphology and neuronal networks

The central nervous system (CNS) is constituted by the brain and the spinal cord, with the brain being located inside the skull, and the spinal cord inside the vertebral canal. The peripheral nervous system (PNS) is external to the CNS and is constituted by sensory receptors and nerves.

The CNS is composed of neurons and non neuronal cells, called glial cells, that account for over half of the brain's weight. Glial cells have several roles such as maintaining the ionic milieu of nerve cells, modulating the rate of nerve signal propagation, modulating synaptic action by controlling the uptake of neurotransmitters at or near the nuclear cleft, etc [4] [5]. The neuron is the functional communication nervous cell, with the ability to receive, process and transmit information; this ability is based in its polarized organization into axons and dendrites [6].

1.2.1 Neuronal morphology

Proper neuronal function depends on forming three primary subcellular compartments: soma, axons, and dendrites [7]. Dendrites receive signals that are processed and integrated at the cell body [8], and structurally they are typically shorter than axons, taper as they leave the cell body, and decrease in diameter as they branch [6] [7]. Dendrites, in contrast to axons, contain polyribosomes and can synthesize proteins, possess specific bungarotoxin-binding sites expressed on their surface, and contain Microtubule-associated protein 2 (MAP2) as one of its microtubule-associated proteins [9].

Additional integration of the signal occurs at the soma [10], where most of the cellular components are produced [7], with this postsynaptic cell integrated response being transferred to the next postsynaptic neuron by the axon [10]. Morphologically, axons possess a diameter relatively constant, which does not decrease with branching [6] [7]. Axons do not have polyribosomes, MAP2, and bungarotoxin receptors, but contain synaptic vesicle-associated proteins and Tau as its microtubule-associated protein [9].

Neurons are usually classified by their structure that is based on the number of processes that extend from the cell body [4].

- *Multipolar neurons* have many dendrites and a single axon. The dendrites vary in number and degree of branching.

- *Bipolar* neurons have two processes, one dendrite and one axon. They are located in some sensory organs, such as in the retina of the eye, and in the nasal cavity.

- *Unipolar neurons* only have a single process extending from the cell body. This process divides into two branches, with one branch extending to the CNS and the other to the periphery.

In this thesis our object of study are cortical primary neurons, which are multipolar neurons cultured "in vitro" upon their dissociation from rat embryos (E18) cortex. These neurons have therefore many dendrites and a single axon.

1.2.2 Neuronal morphology vs function

Neurons are highly specialized cells and the morphological properties of the axonal and dendritic trees are a determinant factor of the neuronal phenotype and maturation level, being essential for neuronal function in network connectivity. The quantitative analysis of neuronal morphology can have important applications to study the relation between neuronal structure and function, to monitor distortions occurring in individual cells or at the network level that may correlate with neurological diseases, and to discover and monitor molecules' ability to influence neuronal differentiation and regeneration in high throughput assays, including specific substances potentially useful for therapeutic drug development [11] [12].

1.2.3 Neuronal differentiation

The establishment of morphological polarity in hippocampal neuronal cells needs seven days in culture, after which the cell displays a characteristic shape, one long axon with relatively uniform diameter, and several dendrites shorter than the axon and with a decreasing diameter. The sequence of events that leads to the establishment of polarity can be divided in five stages [9] [13]:

Stage 1: *Formation of lamellipodia.* Shortly after the cells attach to the substrate, motile lamellipodia start to appear around the cell; their appearance in culture may be a cell adaptation to growth on a 2-dimensional substract. The lamellipodia that initially surrounds most of the cell circumference break up into discrete patches at intervals, along the cell periphery.

Stage 2: *Outgrowth of minor processes.* In this stage the lamellipodia are transformed in distinct processes that will extend to a length of 10-15 μm in a few hours. After they have this length, they exhibit little net elongation, remain motile, and extend and retract short distances. At light-microscope level, all of the minor processes are similar in appearance and growth characteristics. This occurs within the first days in vitro (div).

Stage 3: *Formation and growth of the axon.* After several hours of the appearance of minor processes, one of these starts to grow faster. After this, its rate of growth will be in average 5-10 times greater than the other processes of the cell. This process is the axon and can be identified as soon as its fast growth begins. At this point the cell has become polarized. Some cells develop 2 axons, initially one process begin to growth at a rate typical of axons, then its growth stops and retracts to become a dendrite, and a different process take the axonal characteristics. Several, maybe all, of the initial processes are capable of becoming axons, but when one of them acquires the axonal properties the remaining processes are prevented from becoming axons.

Stage 4: *Growth of dendrites.* Dendrites develop from the minor processes that appear during the first day in culture, but significant dendritic growth begins only after about 4 days in culture, 2-3 days after axonal outgrowth. Unlike the axons, several dendrites grow at the same time, and they growth five times slower than the axon .

Stage 5: *Maturation of axonal and dendritic arbors.* After the axons and dendrites are

morphologically mature, neurons form synaptic contacts that enable the transmission of electrical activity [14]. To achieve the stage five of development, neurons need the presence of synapses, which in turn depend on the presence of several proteins. Among the proteins needed are synaptic vesicle proteins (synaptophysin, synaptobrevin) and plasma membrane proteins (Synaptosomal-associated protein 25 (SNAP-25), syntaxin). Synaptophysin is a glycoprotein within the membrane of presynaptic vesicles and is needed for the exocitosys of synaptic vesicles. Synaptossomal associated protein SNAP-25 is important in docking and fusion of membranes, and its appearance during development is associated with the ability of the neuron to neurotransmission. The expression of SNAP-25 and synaptophysin during development means that the neurons established synaptic contacts.

In this work we have used images of primary neuronal cultures acquired at 4 div (fluorescence images; stage four of differentiation) and 4, 10 and 14 div (phase contrast images; stages four and five of differentiation). These phase contrast images have clear increasing network densities and were therefore useful to test neuritic related parameters.

1.3 Imaging neuronal cells and networks

In order to study neuronal morphology in development and regeneration research areas, neuronal bioimages have to be acquired. They are usually obtained with a microscope and some kind of image digitizing apparatus.

1.3.1 Light microscopy

A light microscope is any microscope that uses visible light to illuminate and image a specimen. This includes white light composed of all wavelengths, as well as the light of a specific wavelength used in fluorescent microscopy, although when someone refers to light microscopy they usually mean nonfluorescent microscopy [15].

The most common and general form of light microscopy is **bright field** microscopy, where the light passes directly through or is reflected off a specimen. It is desirable that the specimen is pigmented to better differentiate structures, and there are several procedures to preserve and stain specimens in order to enhance contrast. However, most of the procedures result in the death of cells to preserve the specimen. Methods of manipulating light to enhance contrast have been developed to make resolvable details observable to the eyes without the application of special dyes[15].

Variations in density within the cells cause tiny differences in the way regions scatter light, because different cellular structures have different index of refraction. **Phase-contrast microscopy** takes advantage of these slight differences, amplifying them into larger intensity differences with high contrast that can be easily seen. Because this does not require special treatment of the specimen to see the many details, phase contrast microscopy is often used to examine cultured cells, including the development of neurons and neuronal networks. Phase contrast microscopy of live cells without staining is therefore

possible and allows the study of living specimens, an advantage in time-course experiments. An example of phase contrast neuronal microphotographs is present in Figure 1.3 [15].

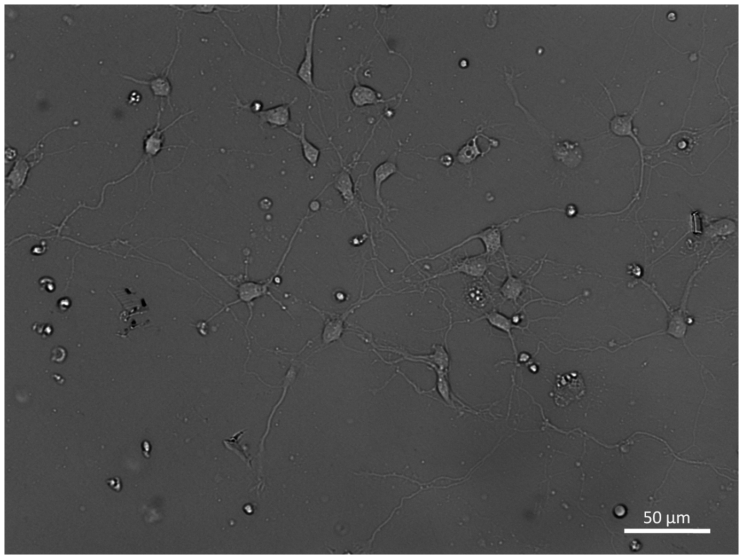

Figure 1.3: Routine phase contrast microscopy bioimage of a cortical primary neuronal 2D culture at 4 div.

1.3.2 Fluorescence Microscopy

Fluorescence microscopy takes advantage of specialized molecules called fluorophores that have the property of absorbing light at a specific wavelength and then emitting it at a different wavelength. Fluorophores can be linked to antibodies or other molecular probes to signal the presence of specific proteins or organelles and mark particular structures within a cell [15].

In fluorescence microscopy the structures tagged with the fluorophores light up against a dark background. Because the background is dark, even a tiny amount of the glowing fluorescent reagent is visible, making fluorescence microscopy a very sensitive technique [15].

However, this technique also has some disadvantages, being the most important one the limited time that fluorescent reagents remain illuminated. The intensity of the light emitted from a fluorophore will decrease overtime as it is continuously exposed to light in a process called photobleaching and, because of this, it is necessary to limit the light exposure of fluorescently tagged specimens and capture their images before the fluorescence becomes too dim. Another limitation is the background noise that can mask the actual signal of interest, with background noise being non-specific and non-meaningful signal. A third important limitation, only occurring in live cell imaging, is phototoxicity, in which illumination (excitation ligth) leads to the death of cells expressing the fluorophore due to free-radical generation.

Fluorescence can be performed by either direct or indirect methods. Direct fluorescence involves the conjugation of the protein of interest at the cDNA level ('fusion protein')or its primary antibody with a fluorophore. In indirect fluorescence the primary antibody is visualized using a fluorophore-conjugated secondary antibody raised against the immunoglobulins of the species in which the primary antibody was raised.

Epifluorescent microscopy is the most used elementary form of fluorescence microscopy. In this technique the specimens labelled with fluorescent probes are illuminated by light of a specific excitation wavelength (or a defined interval of wavelengths). The specimen is viewed using a second filter that is opaque to the excitation wavelength but transmits the longer wavelength(s) of the emitted light, so that the only light transmitted through the eyepiece is the light emitted by the specimen. The major disadvantage of epifluorescence is that excitation light excites fluorophores throughout the entire depth of the specimen and fluorescence signals are collected not only from the plane of focus but also from areas above and below this plane. Such background fluorescence can lead to hazy, out-of-focus images that appear blurry and lack contrast.

Confocal microscopy produces clear images of structures within relatively thick specimens by selectively collecting light from thin regions (the plane of focus) of the specimen. The key aspect of confocal microscopy is that the pinhole aperture in front of the detector is at a position that is confocal with the illuminating pinhole, so only light coming from the same plane in the specimen, where the illuminating light comes to a focus, reaches the detector. This minimizes background fluorescence and maintains a sharp focus on a single plane. The detected light is digitized and sent to a computer for display, storage,

and subsequent manipulation. The major advantage against epifluorescence microscopy is the ability to produce sharp images of cells and cellular structures without background fluorescence. This technique has also disadvantages, since confocal lasers scan specimens point by point to form a complete image of the specimen. This exposes samples to intense light for a longer time period than epifluorescent microscopes, making photobleaching and phototoxicity more problematic. The longer time to capture also makes it less desirable for live cell imaging of extremely fast events. Further, since only the light coming from the same plane in the specimen is collected to form the image, the confocal image is less brighter than epifluorescence images taken with similar excitation light intensities [15].

In general, freely available digital processing tools for neuronal bioimages analysis accept both epifluorescence and confocal fluorescent microphotographs, without any distinction between these types of images.

In our work we will analyse fluorescence microphotographs of cells expressing a known fluorophore, green fluorescent protein (GPP) as shown, for example, in Figure 1.2. In this kind of experimental design one or a few neurons are 'lighted up' against a dark background constituted by non-fluorescing neurons (not expressing the fluorescent protein) and the bottom of the cell plate (when not occupied by cells).

1.4 Aims and structure of the thesis

The underlying work of this thesis focused on the systematic evaluation of digital image processing techniques and tools that may provide insightful and reliable quantitative information regarding neuronal morphology. The first objective was thus to conduct a functional survey of the available relevant software tools for neuronal image processing. A second objective consisted on the development of customized image processing workflows that could handle very specific imaging contexts. Due to the above mentioned peculiarities of phase contrast images, these were selected as the case study for the workflow development.

This thesis is divided in six chapters, with the remaining five chapters organized as follows:

Chapter two *Survey of digital image processing tools for fluorescence neuronal bioimages.*

Begins with a survey of relevant digital tools for neuronal image processing. From this survey three programs were chosen for comparison of their applicability to analyse neuronal fluorescence bioimages (chapter Three). The selected programs' preprocessing requirements were here evaluated.

Chapter three *Benchmarking of digital tools for fluorescence images.*

This chapter presents the results of a functional comparative analysis performed on day-to-day neuronal fluorescence images using the previously selected digital processing tools. Routine epifluorescence neuronal images were used. Data obtained with the various programs was compared to the manual analysis of the images using ImageJ analysis tool [16].

Chapter four *Phase contrast images - Developing new tools.*

In this chapter we have established and optimized a sequence of processing and analysis steps to better extract relevant information of neuronal phase contrast images. For this we have used phase contrast images obtained from rat primary neuronal cultures at various developmental days.

Chapter five *Phase contrast images - A case study.*

The workflow developed in Chapter 4, in the form of an ImageJ macro, was used to answer a scientific question by applying it to phase contrast images of neuronal cultures at increasing differentiating days, in the presence or absence of a relevant pharmacological inhibitor.

Chapter six *Discussion and Conclusion.*

In this chapter the results obtained in the benchmarking analysis of digital tools for fluorescence images are discussed and a workflow for the analysis of this type of images is presented, taking in consideration the specific analytical aims. Results obtained with the newly developed ImageJ macro for neuronal cultures phase contrast images will also be here discussed. Problems that arise during the tools application and that still remain to be answer, and potential future work will also be advanced.

Chapter 2

Survey of Digital Image Processing tools for neuronal images

2.1 Relevant neuronal image features

There are several neuronal morphological characteristics that provide relevant structural information on the neuronal cultures. Neuronal features more relevant for quantitative assessment include cell body (soma) area and circularity, and various neuritic-related parameters such as neuritic length and branching. Soma-related features can be analysed using the following geometrical parameters: maximum diameter (major axis), minimum diameter (minor axis), area, perimeter and shape or aspect ratio (maximum diameter/minimum diameter ratio)[17][3]. Characterization of the neurites can include determining the number of attachment points (neurites directly connected to the cell body), tree length (total neuritic length of a neuron or set of neurons), tree dispersion (geometrical distance between the cell body's center of gravity and the center of gravity of the complete tree) and tree branching (number of end points/number of attachment points ratio) [17] [3].

2.2 Image processing tools - ImageJ and compatible software

Software tools for neuronal digital analysis are capable of quantifying structural parameters in neuronal bioimages, in particular images recorded using light microscopy. The neuronal parameters that these tools can measure vary among the different programs, but generally include[3]:

Primary morphological measurements[1]:

- *Cell body area*, the area of the cell soma;
- *Circularity*, ($4\pi \times area/perimeter^2$) - this value can vary between 1 (perfect circle) and 0 (increasingly elongated shape). The values may not be correct for very small particles;
- *Total neurite length* - the sum of the distances from each neuritic terminal tip to its origin, of all the neurites of all the neurons in the image;
- *Attachment points* - locations where the neurites connect to the soma;
- *Ending points* - the locations at the tips of the neurites.

Secondary measurements[2]:

- *Average cell body area* - total cell bodies' areas divided by the number of neuronal cells;
- *Neurite length per neuron* - the total neurite length divided by the number of neurons in the image;
- *Branching* - the ratio between the number of ending points and the number of attachment points.

Some of the processing components that analyse these parameters were developed to be within the ImageJ software environment. ImageJ is a general purpose image processing program whose name derives from being written in the Java language. This program has its source code openly available and its use is license-free. It can run on any operating system and it is easy to use [16].

ImageJ can read most of the common image formats used in the field of biomedical imaging, such as TIFF, BMP and PNG, among others. It supports all common manipulations, including reading and writing of image files, and operations on individual pixels, image regions, whole images and stacks. It can perform operations such as convolution, edge detection, Fourier transform, histogram and particle analyses (including sophisticated statistical processing of groups of particles), editing and color manipulation. ImageJ also supports more sophisticated operations based on image oriented standard arithmetic and logic operations, and also mathematical morphology operators that are often used in structural filtering of biomedical images [16].

The program's applicability is virtually limitless because of the availability of user written macros and plugins, enabling the user to customize the software environment according to the processing needs raised by the specific analysis problems [16].

[1]parameters usually directly available, normally include: neuronal cell body area, neurite length, attachment points and ending points

[2]parameters calculated using primary measurements

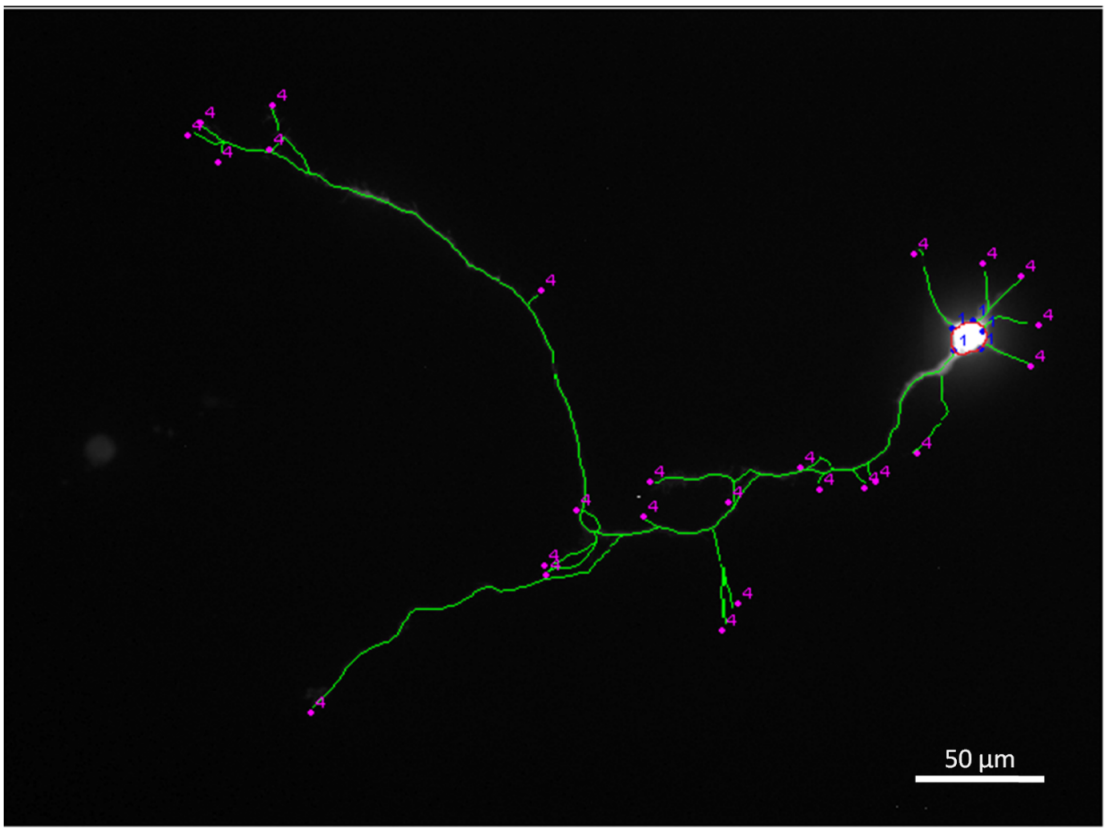

Figure 2.1: Image representing part of the parameters analysed in a neuronal bioimage. Total neurite length is represented in green; in this case, since the image represents a single neuron, green represents both the total neurite length and neurite length per neuron. The ending points are represented in pink. The attachment points are represented by the dots in blue. The cell body is located inside the red area.

Macros are scripts that are meant to ease up the automation of often repeating tasks, which would be tedious to implement manually. ImageJ has an easy-to-use macro-language, meaning that knowledge of Java is not required for writing simple scripts.

Plug-ins are external programs, mostly written in Java language, that offer image processing capabilities that do not exist in the core capabilities of ImageJ and, once implemented, they cannot be distinguished from the program itself. However, developing new plugins requires knowing Java language [16].

There are several publicly available ImageJ plug-ins that are somehow being used in neuronal image processing. For the purpose of this thesis we have selected those that had multiple citations in relevant image processing overview articles [18][3]. The NeurphologyJ [12] and NeuriteQuant [19] software were also included in this comparative analysis since they are the two most recent programs of neuronal morphology quantification reported in the literature that also function in the ImageJ environment.

2.3 Common operations performed by image processing tools

Digital image processing within bioimaging context is usually composed by three main steps: Preprocessing; Segmentation; Feature extraction.

Before the analysis phase it is usually necessary to perform some kind of preprocessing steps on the acquired image raw data in order to improve its visual contents and correct possible defects that may impair the quantitative analysis tasks. Some preprocessing steps usually used are designed to enhance the image contrast, reduce noise and correct illumination problems. After this step of image improvement the image can be segmented (separation of the different components of the image). Pixels with the same characteristics are supposed to be part of the same structure, so segmentation usually starts with an intensity threshold. Morphological filtering is often applied to improve the results. After the segmentation is performed, and the objects are properly separated, quantitative information can be extracted in a procedure called feature extraction.

The main tools of image processing that will be used during this thesis are described below.

Threshold: A grayscale image (with pixels in the range between 0-255) is converted to binary by defining a grayscale cutoff point. Grayscale values below the cutoff become black (0 of intensity value) and those above become white (255 of intensity value). This is useful to separate background data from foreground data including our target objects [20].

Gaussian blur: The application of the Gaussian filter has the effect of smoothing the image. The degree of smoothing is controlled by the choice of the standard deviation parameter sigma. A Gaussian function with a large value of sigma is an example of a so-called low-pass filter in that the sharp edge features (high spatial frequency content) of an image is suppressed [21].

Morphology operators: These use a structural element to probe an image and filtering or quantifying the image according to the manner in which the structural element fits within the image. By marking the locations at which the structural element does fit within the image object(s) we derive structural information about the image, that depends on both the size and the shape of the structural element. This requires that the user defines the type and the radius of the structural element used. The following morphology operations are usually used in image processing and are applied to all the image objects that fit within the structural element:

- The *gray-scale erosion* operation reduces the brightness (and the size) of all bright objects on a dark background in an image, and can be used to eliminate small anomalies from an image, such as single-pixel bright spots, typically smaller than the object(s) of interest.

- The *gray-scale dilatation* operation increases the brightness (and the size) of all bright objects on a black background in an image, and this operation can be used to eliminate small anomalies from an image, such as single-pixel dark spots within or near

the object(s) of interest.

- The *opening operation* is an *erosion operation* followed by a *dilatation operation*, and thus objects tend to maintain their original size. In this, the erosion first eliminates small anomalies such as single-pixel bright spots and reduces the object(s) brightness, and the following dilatation then roughly increases remaining object(s) brightness back to their original levels (and size), roughly eliminating any alterations caused by the previous erosion step on the object(s) of interest. The opening operation is useful to clean up images with noise and other small anomalies related to bright spots. The *Top-hat* image is the image obtained by subtracting a morphologically opened image from the original image.

- The *closing operation* is a *dilatation operation* followed by an *erosion operation*. In this, the dilatation first eliminates small anomalies such as single-pixel dark spots within the object, and the following erosion operation then roughly reduces objects brightness back to their original levels. The closing operation is useful to clean up images with object holes and other small anomalies related to dark spots. The *Bottom-hat* image is the one obtained by subtracting the original image from a morphologically closed version of the image [22].

Skeletonize: The skeleton of a binary object is a representation of the basic form of that object, which has been reduced down to its minimal level. An useful analogy is the "prairie-fire analogy". In this analogy the boundary of an object is set on fire and spreads with uniform velocity in all directions inwards; the skeleton of the object will be defined by the points at which the fire fronts meet and stop each other [20] [23].

2.4 ImageJ Plug-ins

2.4.1 NeuronMetrics

NeuronMetrics is a semi-automated open source[3] software for quantitative analysis of 2D fluorescence images of neurons. It can estimate neurite length, branch number, primary neurite number, territory (the area of the convex polygon bounding the skeleton and cell body), and polarity index, which is the percentage of total length contributed by the primary neurite with the greatest combined length of its trunk and arbor. It is capable of correct branch counts using a method called "faces" in computational geometry [26]. A face is the result of the contact of one neurite with another. Faces are important for the

[3]Open source licenses must permit non-exclusive commercial exploitation of the licensed work, must make available the source code, and must permit the creation of derivative works from the work itself[24]. In opposition proprietary/close source code is kept as a closely guarded trade secret. By maintaining the secrecy of the source code, the software vendor has sole control of its software products, the development of new features, and maintenance[25].

branch count, because when a neurite tip touches another neurite, a false branch point is created [27].[4]

2.4.2 NeuriteTracer

Neurite tracer is an open source plugin that processes pairs of neuronal and nuclear marker 2D images to obtain skeletons of neurites and masks of neuronal nuclei. NeuriteTracer was reported to have a very strong correlation with the values of NeuronJ [28].

The program has some disadvantages, like when closely apposed nuclei are merged into a single nucleus or when non-neuronal cellular nuclei overlap with neurites or cell body, the result is a false positive neuron count. The number of images that can be processed in one batch is limited by the amount of RAM installed in the computer. Further, for accurate tracing the program needs the outgrowth in the images to be well separated; indeed, dense cultures with a great amount of neuritic outgrowth are not traced well because the threshold step merges adjacent neurites[28].

2.4.3 NeurphologyJ

This open source plugin set aims the automate quantification of neuronal morphology from 2D images of fluorescence microscopy. It is capable of quantifying soma number and size, neurite length, attachment points and end points.

NeurphologyJ operates on the entire image, so when an overlapping neurite network is established, it is extremely difficult to identify the origin of a particular neurite. For this reason, NeurphologyJ was not designed to quantify neuronal morphology on a per cell basis. The program does not quantify neurite length on images acquired with high magnification objectives (equal or higher than 40×), since the neurite width in these images is quite large, and when the command 'skeletonize' is applied it produces a tree-like skeleton that results in overestimation of the neurite length. It is also unable to perform ending point quantification on neurons with highly fragmented neurites, because each tip of the neurite fragment will be recognized as ending points [12].

2.4.4 NeuriteQuant

NeuriteQuant is also a freely available open source tool for automated quantification of neuronal 2D morphology. The underlying algorithm performs quantitative measurements of neurite length, neuronal cell body area, neurite-cell body attachment points, and neurite endpoints per field. From these primary measurements it can derive average measurements per neuron for neurite length, cell body area and neurite count.

The program has some limitations, namely: 1) the image analysis is optimal at high signal-to-noise levels, which only enables detection of weak neurite structures by setting

[4]To calculate the territory, the vertices of the skeletonized neuron are connected to form a convex polygon and its area is computed.

low detection thresholds; therefore measurements with markers that stain barely above noise levels are less accurate and weaker neurite structures might be excluded from the analysis by the threshold procedure. 2) At high cell densities, if neuronal cell bodies are not separated from each other, the neuronal cell body number can only be estimated by dividing the total neuronal cell body area by a user-defined reference size of typical neuronal cell bodies. 3) More complex morphometric measurements, which are derived from and/or depend on the ratios of multiple primary morphological measurements like average branch density, are less accurate if only few cells or few small neurite fragments are analysed per field [19].

2.4.5 NeuronJ

NeuronJ is a semi-automatic neurite tracing freeware implemented as a plugin for ImageJ to analyse 2D neuronal fluorescence images. It was compared to fully manual tracing methods (in [29]) and, in terms of length measurements, the differences between NeuronJ and the manual methods were not significant.

NeuronJ tracing is divided in two phases: in the first one (detection phase), to every individual pixel in the image is assigned a value indicating its likelihood of belonging to a neurite; in the second phase (tracing phase), consecutive pixels that are most likely to represent the centerlines of the neurites are linked together to constitute the tracings. The former is a preprocessing step and is carried out fully automatically, the later requires user interaction.

NeuronJ also provides the possibility to label and color tracings, to store them to and load them from disk, and to compute and display the dimensions of individual tracings as well as the statistics of measurements on selected or all tracings [29].

2.5 The MATLAB Environment

MATLAB is a highly regarded software environment for scientific data processing including well integrated computational, programming and visualization functionalities. This is a script oriented environment where programming is actually accomplished through user written files in the form of scripts or functions. These may include core MATLAB functions or special purpose functions normally available within organized, public or commercial, repositories called toolboxes [30]. A major distinguishing feature of MATLAB is its core array processing design. Every object is a "matrix" and all sorts of operations are array oriented. Images are data structures that match well with MATLAB approach to data processing. MATLAB based image processing is a lively area of software development and, besides its own toolbox, there are many tools available to tackle the very wide scope of problems arising in image processing. Neuronal image processing is no exception and, in the following sections, we will briefly mention representative MATLAB based tools. Although the MATLAB learning curve is generally steep, the programming skills for the common user in the bioimaging field are still demanding and time consuming. This par-

tially justifies the prevalence of solutions based on ImageJ tools, reinforced by the fact that they are commonly open source and publicly available free of charge.

Programs that function in MATLAB environment

2.5.1 Neuroncyto

The open source software Neuroncyto is fully automated and can measure neurite length on a cell-by-cell basis, the branching complexity of a neurite[5], and the number of neurites per cell. This software uses topological analysis to segment the cells. The image analysis algorithms were developed for images acquired by two-channel microscopy but can be applied to cellular images of multichannel microscopy if the nuclei are acquired by one of the channels [31].

2.5.2 Edge-based tracing

This is a novel algorithm implemented in MATLAB and was used to analyse images acquired using multi-channel fluorescence microscopy. It is designed for the automatic labelling and tracing of branching structures and it does this by tracing and extracting the center line points recursively, detecting the edge points for each line in the image; the tracing results are then smoothed out using a 2D curve smoothing method, to remove jaggy-looking traces while preserving the line structures. The algorithm is capable to detect soma and measure parameters such as the length per neurite and total neurite length. The quantitative evaluation of the tracing performance of the algorithm shows that the results generated by the algorithm are similar to those generated by two independent observers that labelled the images manually[32].

Standalone tools

2.5.3 Dynamic programming

Dynamic programming[6] is an automatic algorithm for extraction of neurites that labels all the neuritic segments of neurite structures in fluorescence neuronal images. The algorithm selects the starting and ending points automatically, by iteratively tracing the centerline points along the line path representing the neurite segment. Of note, the time needed to extract the neurite structures in an image with the size 1360×1200 is 24.1 seconds in a PC with Pentium IV, 2.4GHz and 1024 MB memory [33].

[5] the number of the branches of that neurite divided by the length of the neurite.

[6] actually the program does not have a name, having this designation since it is based in this methodology.

2.5.4 Multineurite

This is an automated freeware for neurite analysis requiring user interaction in setting initial parameters. The program is designed to analyse 2D fluorescence microscopy images. It is able to generate branching and endpoints and mark all neurites, but without classifying them into the neurons they belong to; this occurs due to the growth of neurons in clusters and the difficulty to identify neurites from individual neurons in some images. The algorithm consists on two phases: the first one is the marking phase, in which a multi-scale curvilinear structure detector, based on the local Hessian matrix, yields a single and connected response to each neurite; in the second phase, the program connects near branching structures that are broke[1].

A summary of all these programs and the morphological parameters they can measure is shown in Tables 2.1 and 2.2, together with information about their license type.

Table 2.1: Resume of characteristics of the programs listed above. The number of citations in peer reviewed papers was obtained by the search engine 'Google'.

Program	Freeware	Open source	Times cited in peer reviewed papers
NeuronMetrics	yes	yes	23
NeuriteTracer	yes	yes	42
NeurphologyJ	yes	yes	2
NeuriteQuant	yes	yes	0
NeuronJ	yes	no	342
Multineurite	yes	no	49
NeuronCyto	yes	yes	29
Edge-based tracing	no	no	35
Dynamic programming	no	no	23

From the programs listed in Tables 2.1 and 2.2, NeurphologyJ, NeuriteQuant and NeuronJ were selected to be used in benchmarking tests with our fluorescence images. These programs were chosen because NeurphologyJ and NeuriteQuant are the two most recent programs of neuronal morphology quantification reported in the literature, both are open source, work in ImageJ, a single image of fluorescence microscopy is sufficient to measure neurite outgrowth, and are automatic. NeuriteTracer was not chosen since it requires pairs of fluoresce images that include the nuclei, and NeuronMetrics was put aside since it is semi-automatic. NeuronJ is usually used as control to compare the results from other freewares tools since the program is semi-automatic and its results are reported to be similar to the ones obtained by manual analysis. Further, NeuronJ is the most widely used freeware for neuronal analysis, as shown by its higher number of citations (Table 2.1).

Table 2.2: Resume of the relevant characteristics of various programs available for analysis of fluorescence neuronal microphotographs.

Program	Morphology related parameters evaluated	Compatibility with ImageJ	Authors
NeuronMetrics	Total neurite length; branch number estimate; primary neurite number; territory and polarity index	yes	Narro et al, 2007
NeuriteTracer	Count neuronal nuclei; traces and measures Neurite Length	yes	Pool et al, 2008
NeurphologyJ	Soma number and size; neurite length; neurite attachment and ending points	yes	Ho et al. 2011
NeuriteQuant	Total neurite length; total neuronal cell Body area; average cell body cluster size; total number of cell bodies; number of neurite endpoints; quantification of the average signal intensity; total branch number; branch density along the neurite length; average neurite length per neuron; average length of individual neurites	yes	Dehlmelt et al, 2011
NeuronJ	Length per neurite; total neurite length	yes	Meijering et al, 2004
Multineurite	Neurite length; branching and endpoints	N/a	Xiong et al, 2009
NeuronCyto	Length of neurites on a cell-by-cell basis; branching complexity; number of neurites	no, MATLAB	Yu et al, 2007
Edge-based tracing	Soma detection; length per neurite and total neurite length	no, MATLAB	Zhang et al, 2007
Dynamic programming	Length of total neurite segments	N/a	Zhang et al, 2007

N/a- Information not available

2.6 The need for pre-processing

Before performing the benchmarking test the programs were applied to both raw images and images that were pre-processed to enhance contrast and correct for non-uniform illumination effects. The objective was to evaluate if the selected programs are ready to analyse our raw images or if some type of pre-processing was needed.

2.6.1 Pre-processing tasks

To enhance the contrast of our neuronal fluorescence images we used the method proposed in [32] that is mostly based on gray-scale mathematical morphology concepts [34] using the Top and Bottom hat transformations. Technically, the top-hat transform subtracts a morphologically opened image from the original image, while the bottom hat transform subtracts the original image from a morphologically closed version of the image. Using the top-hat transforms it is possible to detect object crests, while using the bottom-hat transform we emphasize the object's valleys. In our images, the structural element used to both the open and close operations was a circle with size four pixels, since this is roughly the typical diameter of the proximal region of the neurites (attachment points) in these images. These authors propose to add the top hat transformed image to the original image and then subtract the bottom hat transform. In order to correct illumination we used a method similar to the proposed by Leong, et al [35]. The idea is to estimate an approximation of the background intensity function. This is accomplished by computing a lowpass-filtered version of the image and subtracting it from the original. In order to obtain a reasonable approximation for the background behaviour, the filter is normally build upon a large Gaussian kernel with the standard deviation above 120 pixels. In Figures 2.2b and c it is possible to observe the effects of these pre-processing steps in opposition to the original image (Figure 2.2a).

The following three fluorescence images (Figure 2.3a, b and c) were used as case studies for the need of preprocessing operations before the application of the selected digital programs (NeuronJ, NeurphologyJ and NeuriteQuant).

(a) Unprocessed image.

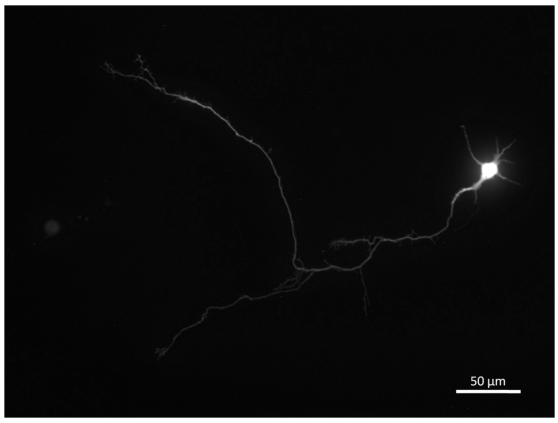

(b) Previous image with its contrast enhanced through morphology operations (see text above).

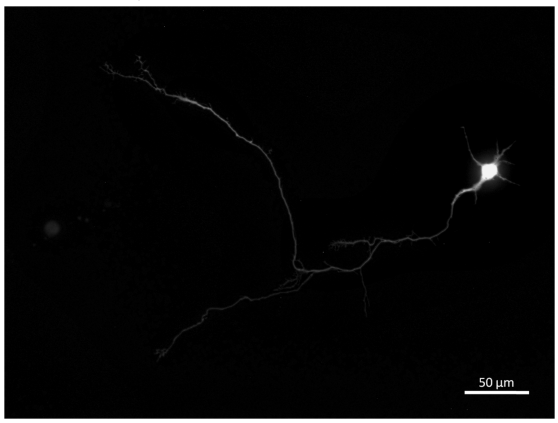

(c) Previous image following illumination correction using a Gaussian Blur with radius 100.

Figure 2.2: Image used to examplify the alterations arising from the described preprocessing operations.

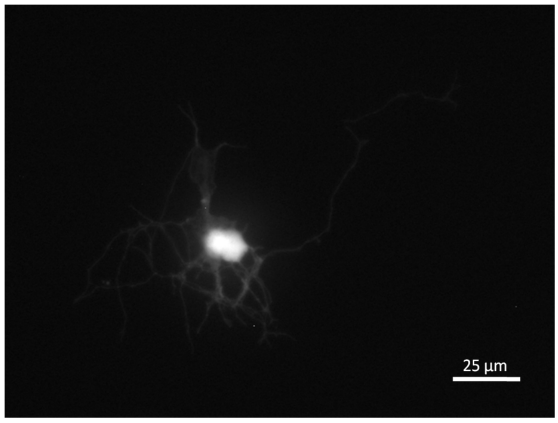

(a) Raw image a.

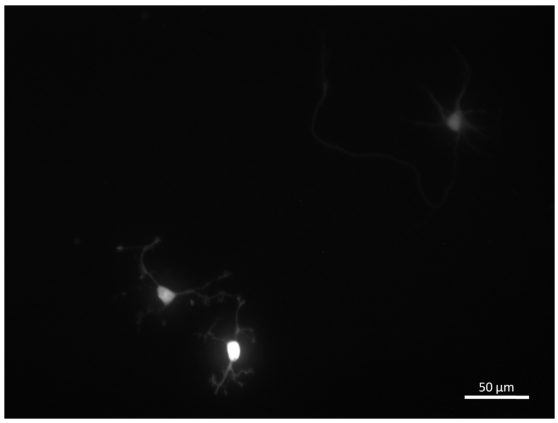

(b) Raw image b.

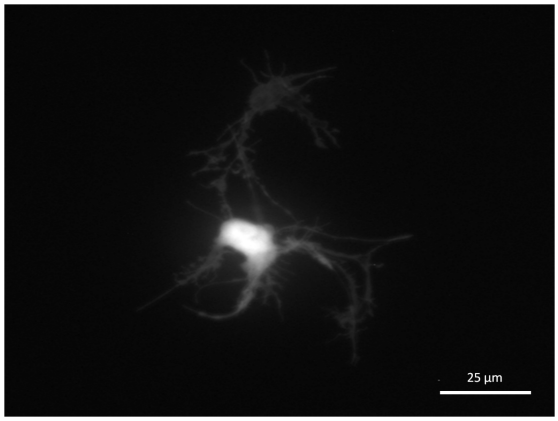

(c) Raw image c.

Figure 2.3: Raw neuronal fluorescence images used to assess the importance of preprocessing before using the selected analytical software.

2.6.2 Preprocessing in NeurphologyJ

The program uses pre-processing to increase the signal-to-background ratio. It uses three functions to achieve image enhancement, which are: edge detection, uneven background correction and intensity-based pixel selection. The program will be used to analyse fluorescence images such as the example images a, b and c in Figure 2.3, before and after being preprocessed by manually applying the preprocessing tasks described in the 2.6.1 section.

As shown in Figures 2.3a, 2.4a and 2.4b the cell body is well detected in both cases, however the neurites are fragmented and some are not even marked. The image without pre-processing 2.4a has its neuritic network clearly sub-measured and in the preprocessed image of Figure 2.4b most of the thin and dim neurites are not marked.

(a) Image a.

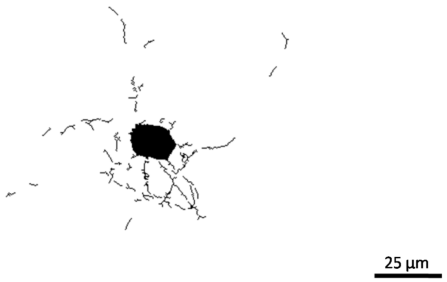

(b) Image b.

Figure 2.4: Neuronal fluorescent image 2.3a analysed with (image b) and without (image a) preprocessing in NeurphologyJ.

For the second example we can compare images in Figures 2.3b (original image), 2.5a (raw image analysed with NeurpholyJ) and 2.5b (image analysed with NeurphologyJ with previous preprocessing). In both the images analysed by NeurphologyJ one cell and its

neurites are missing. In the image obtained upon analysis of the raw image, one of the cells has no neurites marked, and in the other cell there are gaps within the neurites. In the case of the preprocessed image 2.5b, the neurites are better recognized, but the dim and thin neurites are still absent from the final image, not being detected by the program.

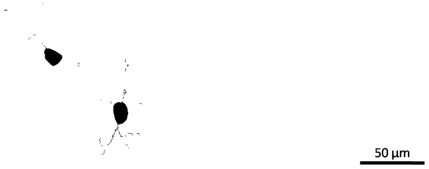

(a) Image a.

(b) Image b.

Figure 2.5: Neuronal fluorescent image 2.3b analysed with (image b) and without (image a) preprocessing in NeurphologyJ.

In the third example we can compare the original image (Figure 2.3c) with the ones obtained with NeurphologyJ with (Figure 2.6b) or without (Figure 2.6a) preprocessing. The cell body is correctly marked in both the Figure 2.6 images. In the raw image 2.6a the neurites are much more fragmented and the network is clearly submeasured. The neurites in the preprocessed image 2.6b have some gaps along the neurites, causing a small subestimation in neurite length.

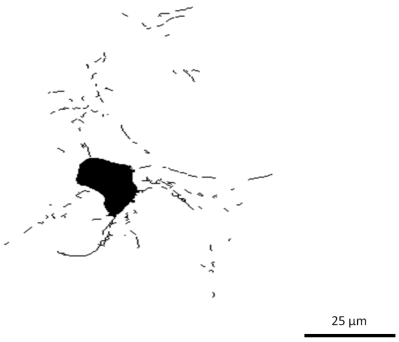

(a) Image a.

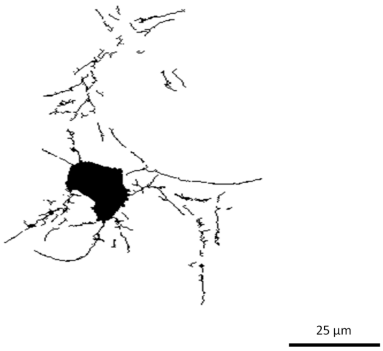

(b) Image b.

Figure 2.6: Neuronal fluorescent image 2.3c analysed with (image b) and without (image a) preprocessing by NeurphologyJ.

2.6.3 Preprocessing in NeuriteQuant

The program NeuriteQuant does not perform any pre-processing to the images before analysing them[19].

In the first case analysed with NeuriteQuant, in the image without preprocessing (Figure 2.7a) it is possible to see that the neurites are marked correctly, but the thin and dim neurites possess some gaps. Imposing pre-processing, as shown in Figure 2.7b results in the overestimation of neurites, due to the huge area marked around the soma. It is also possible to see a gap in the longest neurite.

(a) image a.

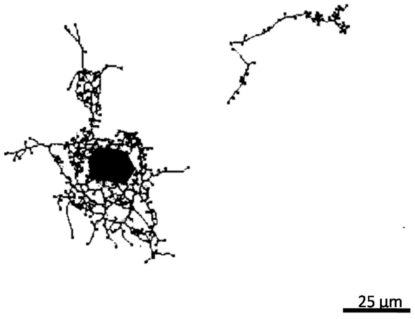

(b) image b.

Figure 2.7: Neuronal fluorescent image 2.3a analysed with (Image b) and without (image a) preprocessing by NeuriteQuant.

In the group of images of Figures 2.3b (original image) and 2.8a and 2.8b (second example of NeuriteQuant application), in the raw image, Figure 2.8a the cell with less contrast and its neurites are not recognized; further, the neurites of the recognized cells present a few gaps, and dim and thin neurites are not recognized. The processed image in Figure 2.8b has all its cells marked, but there is a small gap in the cell with lower

contrast. The other two cells have all their neurites correctly marked, with no gaps, and more neurites are visible than in the unprocessed image.

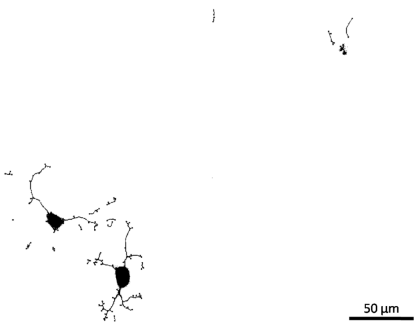

(a) image a.

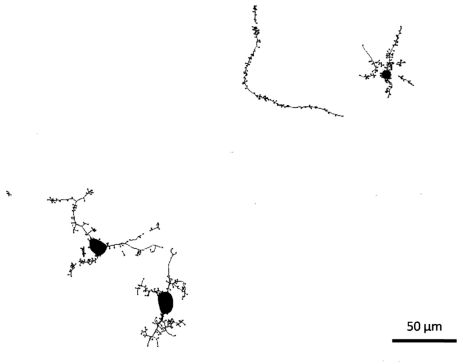

(b) image b.

Figure 2.8: Neuronal fluorescent image 2.3b analysed with (Image b) and without (Image a) preprocessing by NeuriteQuant.

In the group of images of Figure 2.3c (original image), and 2.9a and 2.9b (third example) the raw image (Figure 2.9a) presents a gap in an area that has low contrast, and some endpoints and small branches are not recognized. In the processed image the neurites are correctly marked, and some small neurites not marked in Figure 2.9a are already marked in this image, leading to an increase in the network area.

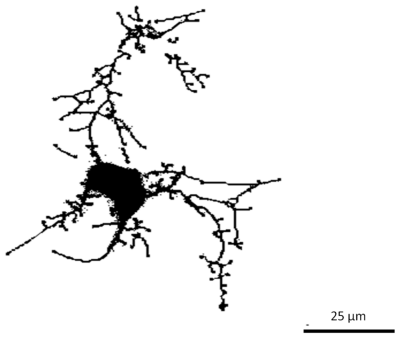

(a) image a.

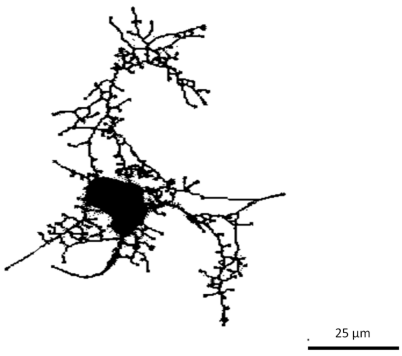

(b) image b.

Figure 2.9: Neuronal fluorescent image 2.3c analysed with (image b) and without (image a) preprocessing by NeuriteQuant.

2.6.4 Preprocessing in NeuronJ

NeuronJ is a semi-automatic program that requires user interaction to trace the neurites. To analyse the images first we have to open the plugin NeuronJ in *Plugins/NeuronJ*, after which the image is loaded in *Load image/tracings* and the command `Add tracings` is used to draw the neurites. After all the neurites are draw the command *Measure tracings* is used to obtain the neuritic length. NeuronJ gives similar or equal results with or without preprocessing, since it mainly depends on manual draw. Figure 2.10 shows examples of images (originals in Figure 2.3) analysed with NeuronJ, where the neurites were drawn in an semi-automatic manner, since the program depends on the manual determination of several points along the neurite.

2.6.5 Manual analysis (using ImageJ)

In Figure 2.11 it is possible to observe the example images of Figure 2.3 with a method further described in detail in Chapter 3 used to analyse images manually using the ImageJ drawing tools.

(a) image a.

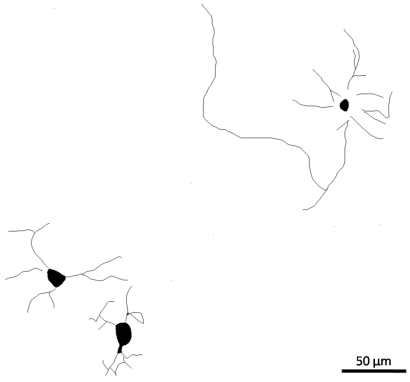

(b) image b.

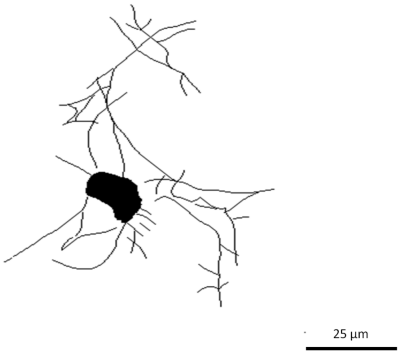

(c) image c.

Figure 2.10: Example images of figure 2.3(a, b and c) analysed with the program NeuronJ.

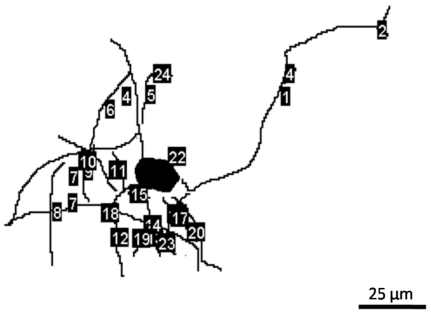

(a) Image a.

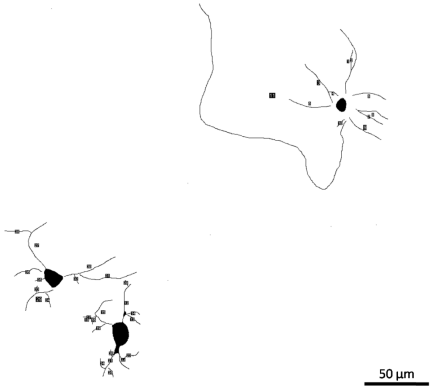

(b) Image b.

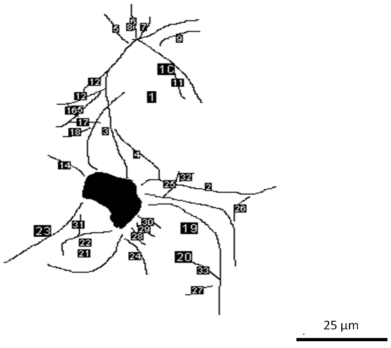

(c) Image c.

Figure 2.11: Example images analysed with the program ImageJ.

2.6.6 Concluding remarks

From the survey of freeware tools that analyse fluorescence images NeurphologyJ and NeuriteQuant were chosen since these programs are automatic, only need a single image of fluorescence microscopy to measure neurite outgrowth, and are both open-source. NeuronJ was chosen since it is the most used program and is also used as a measure of comparison when new digital analytical programs are tested.

About the need for preprocessing, this apparently improved the identification of neurites (and therefore the following segmentation step) for both softwares. However, it created a high number of false positive neurites in NeuriteQuant. Further, preprocessing was not able to resolve the problem of NeurphologyJ to detect thin and dim neurites. Hence the need for preprocessing will be further tested by the full application of the selected programs (Chapter 3). Further, it is not possible to generalize the scope of a tool since its appropriateness depends on the need of preprocessing, the efficiency of this preprocessing, and the quality of our raw data, which is often acquired in quite diverse experimental and technical conditions.

Chapter 3

Benchmarking of digital tools for fluorescence images

In this chapter we present the quantitative results obtained with the analysis of routine fluorescence images using with the programs chosen in the previous chapter.

3.1 Manual analysis

The control further used for all the freeware programs tested consisted on data extracted from a manual analysis of the fluorescence images. Nine images, in a total of 12 cells, were analysed by one observer. ImageJ was the program used to visualise the images and to perform the manual drawing of relevant features, such as neurites and cell bodies. Fluorescence images were analysed with ImageJ using the tool *Freehand line* to draw the neuronal contours. To measure the neurites the command *Measure* was used, followed by the command *Label* to mark the neurites that were being measured. When all neurites are marked, the column 'Length' in the results window is summed to obtain the Total Neurite Length. To measure the Cell Body Area we used the command *Magnifying glass* to increase the zoom in the cell body, then the command *Freehand selections* was used to delineate the cell body manually. After the selection, the command *Create mask* was used; in the mask a threshold is set to select the area corresponding to the cell body, and then the command *Analyse particles* was used to retrieve quantitative data from the cell body. In order to count the attachment and ending points, the plugin *cell counter* was used. With this plugin the points of interest are manually marked by the user, and labelled and stored by the program; of note, up to 8 types of markers are available from the program.

In Table 3.1 is possible to observe that the mean Number of Cells in the fluorescence images is 1.3 ± 0.2 and the mean Cell Body Area per Cell is 141.4 ± 13.8 μm^2. A wide range of Cell Body Area values is present in this set of images, with the maximum in image 4 (237.8 μm^2) and the minimum in images 3 and 9 (99.3 μm^2). The mean Neurite Length per Cell is 602.7 ± 114.8 μm, with a maximum of 1291.9 μm (image 5), and a minimum of 249.7 μm (image 9), thus also presenting a large range. The number of Attachment Points

Table 3.1: Parameters obtained with the manual analysis of fluorescence images of neuronal primary cultures at 4 div.

Image	Number of Cells	Cell Body Area	Neurite Length per Cell	Total Neurite Length	Attachment points	Ending points	Branching
1	1	117.6	965.8	965.8	5.0	34.0	6.8
2	1	142.2	624.2	624.2	7.0	29.0	4.1
3	1	99.3	271.6	271.6	7.0	21.0	3.0
4	1	237.8	656.5	656.5	11.0	33.0	3.0
5	1	131.1	1291.9	1291.9	10.0	24.0	2.4
6	3	139.5	351.9	1055.8	5.0	15.0	3.0
7	1	152.7	399.4	399.4	10.0	22.0	2.2
8	1	153.4	612.9	612.9	11.0	39.0	3.5
9	2	99.0	249.7	499.4	6.0	15.5	2.6
Mean	1.3	141.4	602.7	708.6	8.0	25.8	3.4
SEM	0.2	13.8	114.8	110.3	0.8	2.8	0.5

is 8.0 ± 0.8 and the number of Ending points is 25.8 $\pm$2.8. Finally, the mean Branching of these images corresponds to 3.4 ± 0.5.

Table 3.2: Parameters obtained with the semi-automatic freeware program NeuronJ from the analysis of fluorescence images of neuronal primary cultures at 4 div.

Image	Number of Cells	Neurite Length per Cell	Total Neurite Length
1	1	977.7	977.7
2	1	707.4	707.4
3	1	310.6	310.6
4	1	654.8	654.8
5	1	1281.3	1281.3
6	3	350.9	1052.6
7	1	423.5	423.5
8	1	629.7	629.7
9	2	255.2	510.3
Mean	1.3	621.2	727.6
SEM	0.2	112.7	105.6

3.2 NeuronJ

NeuronJ is a semi-automatic program that only allows to draw neurites (with user interaction) and quantify their length. In the analysis with NeuronJ the mean Neurite Length per Cell is of 621.2 $\pm$112.7 μm, a value that is close to the manual analysis (602.7$\pm$ 114.8 μm) (Table 3.2). Assuming normally distributed data (since the results passed the

Kolmogorov-Smirnov normality test) an unpaired t test shows that there is no statistically difference of the means obtained using ImageJ and manual analysis (Figure 3.2).

Table 3.3: Parameters obtained with the freeware program NeurphologyJ from the automatic analysis of raw fluorescence images of neuronal primary cultures at 4 div.

Image	Number of Cells	Cell Body Area	Neurite Length per Cell	Total Neurite Length	Attachment points	Ending points	Branching
1	2	116.0	351.3	702.6	4.5	99.0	22.0
2	1	156.9	133.9	133.9	2.0	122.0	61.0
3	1	134.4	104.5	104.5	3.0	69.0	23.0
4	1	275.0	308.1	308.1	6.0	149.0	24.8
5	1	169.6	461.3	461.3	13.0	464.0	35.7
6	2	144.0	43.2	86.5	1.5	34.5	23.0
7	1	252.0	267.4	267.4	8.0	159.0	19.9
8	1	213.9	249.0	249.0	5.0	190.0	38.0
9	2	104.3	122.7	245.5	3.0	93.0	31.0
Mean	1.3	174.0	226.8	284.3	5.1	153.3	30.9
SEM	0.2	20.0	45.2	65.0	1.2	42.0	4.3

3.3 NeurphologyJ in raw images

In the raw images, NeurphologyJ presented a similar Number of Cells as the manual analysis (1.3). Nonetheless, the program has marked false positive cells (image 1: 2 cells are marked when only one is present) and false negative cells (image 6: 2 cell was marked when 3 were present). The mean of Cell Body Area is 174.0 $\pm$20.0 μm^2, not statistically different from the manual analysis (Figure 3.1). The mean Length per Cell is 226.8 $\pm$45.2 μm, a value statistically different from the manual analysis (602.7 $\pm$ 114.8 μm, p<0.001)(Figure 3.2). This lower value is due to the lack of sensitivity of the program to detect the neurites, as it is possible to observe in the Figures 2.4a, 2.5a and 2.6a (Chapter 2). The mean Number of Attachment points is 5.1 $\pm$ 1.2 slightly lower than control, but not found to be statistically different (Figure 3.3). The mean value of Ending points is 153.3 $\pm$ 42.0 and the mean Branching is 30.9 $\pm$ 4.3, with both values being significantly higher than in manual analysis (Figures 3.4 and 3.5).

3.4 NeurphologyJ in preprocessed images

Concerning the Number of Cells, even after preprocessing, NeurphologyJ continued to mark a false negative cell in image 6, although correcting the error occurred in image 1 (Table 3.4). Thus, the mean Number of Cells is 1.2$\pm$0.2, which is under the manual analysis mean (1.3 $\pm$ 0.2). The Cell Body Area is much higher (197.8 $\pm$ 22.8 μm^2) than in manual analysis (141.4 $\pm$ 13.8 μm^2), but still the difference was considered not quite significant

Table 3.4: Parameters obtained with the freeware program NeurphologyJ from the automatic analysis of enhanced fluorescence images of neuronal primary cultures at 4 div.

Image	Number of cells	Cell Body Area	Neurite Length per Cell	Total Neurite Length	Attachment points	Ending points	Branching
1	1	244.2	901.0	901.0	12.0	141.0	11.8
2	1	160.7	297.4	297.4	7.0	133.0	19.0
3	1	138.1	183.5	183.5	6.0	62.0	10.3
4	1	305.0	409.4	409.4	17.0	100.0	5.9
5	1	175.3	590.3	590.3	13.0	346.0	26.6
6	2	148.0	126.6	253.2	4.0	48.5	12.1
7	1	281.6	336.5	336.5	13.0	106.0	8.2
8	1	220.1	513.5	513.5	11.0	197.0	17.9
9	2	107.2	216.6	433.2	8.0	100.0	12.5
Mean	1.2	197.8	397.2	485.5	10.1	137.1	13.8
SEM	0.1	22.8	80.8	11.9	1.4	29.9	2.1

(p=0.0503) using the Mann-Whitney test (Figure 3.1). The mean Neurite Length per Cell is 397.2 $\pm 80.8 \mu m$, a value far from the manual analysis (602.7 ± 114.8 μm), but still not statistically significant using the two-tailed Unpaired t test (p=0.1627) (Figure 3.2). The mean number of Attachment points (10.1 ± 1.4) is close to the manual analysis (8.0 ± 0.8) (Figure 3.3). The mean Number of Ending points is 137.1 ± 29.9, far from the manual analysis (25.8 ± 2.8). This clear overestimation of the Ending Points is due to the fragmentation of the neurites and gaps between them, which may be caused by the low accuracy of the program to detect the neurites in these images, since each fragment created has two ending points that contributes to the increase in this value (Figure 3.4). The mean branching is 13.8 ± 2.1, significantly higher than in manual analysis (3.4 ± 0.4) (Figure 3.5), as expected from the results regarding the number of Ending Points.

Table 3.5: Parameters obtained with the freeware program NeuriteQuant from automatic analysis of raw fluorescence images of neuronal primary cultures at 4 div.

Image	Number of Cells	Cell Body Area	Neurite Length per Cell	Total Neurite Length	Attachment points	Ending points	Branching
1	1	163.0	1034.2	1034.2	4.0	105.0	26.3
2	1	128.2	516.1	516.1	5.0	103.0	20.6
3	1	106.7	231.0	231.0	5.0	40.0	8.0
4	1	198.9	488.1	488.1	8.0	68.0	8.5
5	1	124.2	1642.9	1642.9	13.0	399.0	30.7
6	2	109.1	225.8	451.6	6.0	52.0	8.7
7	1	222.1	403.5	403.5	6.0	50.0	8.3
8	1	165.5	641.9	641.9	6.0	115.0	19.2
9	2	79.9	357.4	714.8	5.0	82.5	16.5
Mean	1.2	144.2	615.7	680.5	6.4	112.7	16.3
SEM	0.1	15.5	152.2	141.9	0.9	36.9	2.8

3.5 NeuriteQuant in raw images

In the analysis of raw images with NeuriteQuant (Table 3.5), the mean Number of Cells per image is 1.2 ± 0.1, slightly lower than in manual analysis since one cell is not marked in image 6. The mean Cell Body Area is 144.2 ± 15.5 μm^2, a value very close to manual analysis (141.4 ± 13.9 μm^2) (Figure 3.1). The mean Neurite Length per Cell is 615.7± 152.2 μm, which is also close to the manual analysis (602.7 ± 114.8 μm) (Figure 3.2). The mean number of Attachment points is 6.4 ± 0.9, and is slightly lower than the value of manual analysis 8.0 ± 0.8 (Figure 3.3). The Ending point (112.7 ± 36.9) and Branching (16.3 ± 2.8) values are higher than in manual analysis (Figures 3.4 and 3.5), although being the ones more similar to the control manual analysis. Again, this is probably due to the overestimation of the number of Ending Points by the fragmentation of the neurites and some wider gaps present along the neurite; it may also be due to counting small protusions of the neurites not clearly distinguished by the human observer, as ending points.

Table 3.6: Parameters obtained with the freeware program NeuriteQuant from automatic analysis of enhanced fluorescence images of fluorescence of neuronal primary cultures at 4 div.

Image	Number of Cells	Cell Body Area	Neurite Length per Cell	Total Neurite Length	Attachment points	Ending points	Branching
1	1	215.4	1584.8	1584.8	5.0	243.0	48.6
2	1	169.0	1039.0	1039.0	14.0	155.0	11.1
3	1	140.1	416.5	416.5	10.0	81.0	8.1
4	1	310.5	766.1	766.1	14.0	101.0	7.2
5	1	184.6	2964.2	2964.2	16.0	480.0	30.0
6	3	115.1	430.0	1290.0	6.3	85.0	13.4
7	1	311.0	495.8	495.8	11.0	58.0	5.3
8	1	226.5	913.9	913.9	15.0	113.0	7.5
9	2	106.6	860.2	1720.3	12.0	114.5	9.5
Mean	1.3	197.6	1052.3	1243.4	11.5	158.9	15.6
SEM	0.2	25.3	268.2	261.6	1.3	44.0	4.8

3.6 NeuriteQuant in preprocessed images

In the images analysed after preprocessing the mean Number of Cells is 1.3 ± 0.2, with all cells marked correctly (Table 3.6). The Cell Body Area is 197.6±25.3 μm^2, a value much higher than in manual analysis but still considered not statistically significant (p=0.1135) due to its high error SEM (SEM of 13%) (Figure 3.1). The mean value of Neurite Length per Cell is 1052.3 ± 268.2 μm, a value higher than in manual analysis (602.65 ± 114.80 μm). However, the difference is considered not statistically significant using the test Mann-Whitney Test (Figure 3.2). The mean values of Attachment points (11.5 ± 1.3), Ending points (158.9±44.0) and Branching (16.6±4.8) are higher than in manual analysis (Figures

3.3, 3.4 and 3.5), probably due to apparently false positive neurites marked around the cell body that were previously observed to arise from the processing step (Figure 2.7).

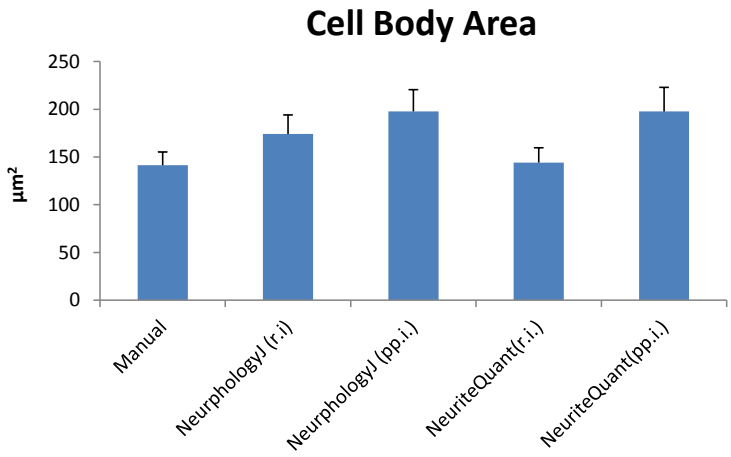

Figure 3.1: Graphic with Cell Body Area of fluorescence microscopy images of GFP transfected neuronal primary cultures at 4 div. ri, raw images; ppi, pre-processed images. Non-parametric methods were used to test for statistic significant differences since not all data passed the Kolmogorov-Smirnov (K-S) normality test. Differences between all groups were tested using the Kruskal-Wallis test (a non-parametric ANOVA), and no significant differences were found. Using non-parametric Mann-Whitney test to separately compare the programs with the manual analysis we have found not quite significant differences only for NeurphologyJ/ppi (p=0.0519).

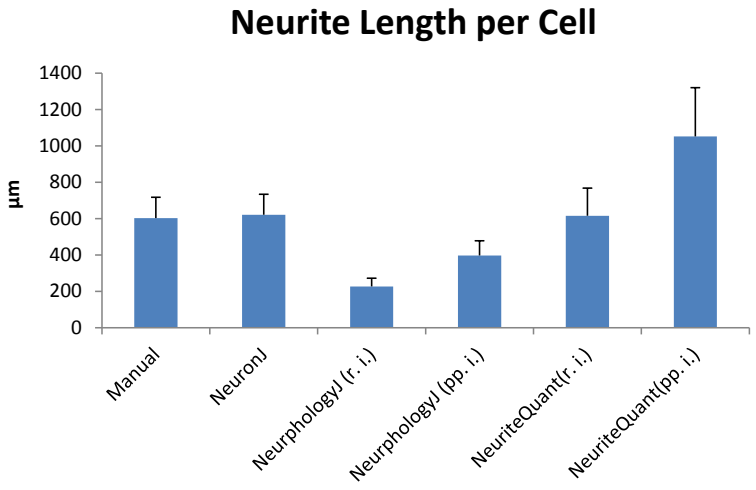

Figure 3.2: Graphic with the Neurite Length per Cell of fluorescence microscopy images of neuronal primary cultures at 4 div. ri, raw images; ppi, pre-processed images. Non-parametric methods were used to test for statistic significant differences since not all data passed the K-S normality test. Differences between all groups were tested using the Kruskal-Wallis test (a non-parametric ANOVA), followed by the Dunn test if $p<0.05$. Differences obtained were for NeurphologyJ/ri: $p<0.05$ vs manual analysis; $p<0.01$ vs NeuronJ; $p<0.001$ vs NeurphologyJ/ppi.

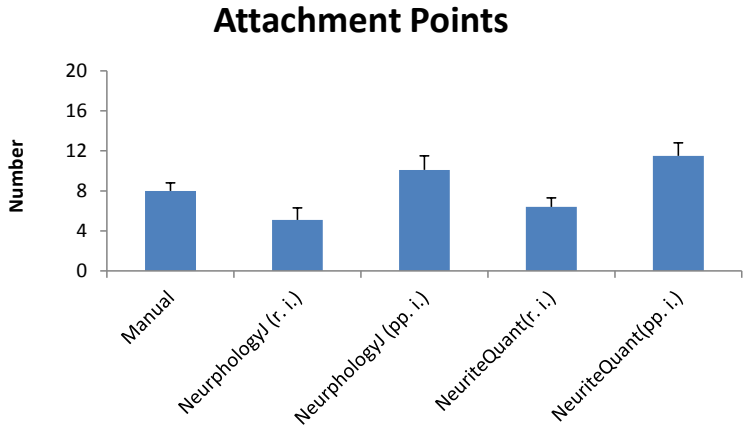

Figure 3.3: Graphic with the mean Attachment points per the cell of fluorescence microscopy images of neuronal primary cultures at 4 div. ri, raw images; ppi, pre-processed images. Non-parametric methods were used to test for statistic significant differences since not all data passed the K-S normality test. Differences between all groups were tested using the Kruskal-Wallis test (a non-parametric ANOVA), followed by Dunn test if $p<0.05$. Significant differences were found only for NeurphologyJ/ri vs NeuriteQuant/ppi ($p<0.01$). Using non-parametric Mann-Whitney test to separately compare each of the programs with the manual analysis we have found not quite significant differences between NeuriteQuant/ppi ($p=0.0504$), and significant differences for NeurphologyJ/ri ($p<0.05$.)

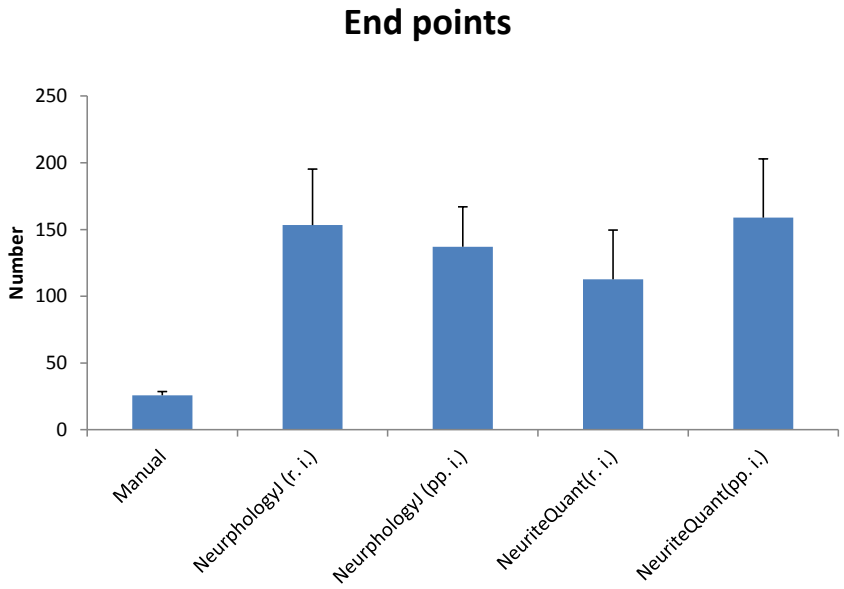

Figure 3.4: Graphic with the mean Ending points per cell of fluorescence microscopy images of neuronal primary cultures at 4 div. ri, raw images; ppi, pre-processed images. Non-parametric methods were used to test for statistic significant differences since not all data passed the K-S normality test. Differences between all groups were tested using the Kruskal-Wallis test (a non-parametric ANOVA), followed by the Dunn test if $p<0.05$, with differences being found for manual analysis vs all the programs: NeurphologyJ/ppi ($p<0.01$); NeurphologyJ/ri ($p<0.01$); NeuriteQuant/ppi ($p<0.001$); NeuriteQuant/ri ($p<0.05$).

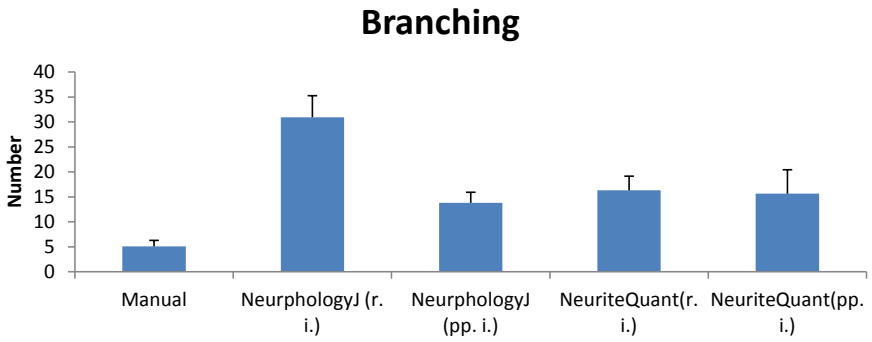

Figure 3.5: Graphic with the mean Neurite Branching per cell of fluorescence microscopy images of neuronal primary cultures at 4 div. ri, raw images; ppi, pre-processed images. Non-parametric methods were used to test for statistic significant differences since not all data passed the K-S normality test. Differences between all groups were tested using the Kruskal-Wallis test (a non-parametric ANOVA), followed by the Dunn test if $p<0.05$, with differences being found for manual analysis vs: NeurphologyJ/ppi ($p<0.05$); NeurphologyJ/ri ($p<0.001$); NeuriteQuant/ri ($p<0.01$).

3.7 Concluding remarks

Preprocessing did not affect the extraction of number of cells, resulted in a overestimation of cell body area, increased the neurite length per cell and the number of attachment points. Both programs tested greatly increased the number of ending points and branching. From all the previous data it is possible to observe that none of these automatic freeware tools is capable of perfectly analyse our neuronal fluorescence images. Nonetheless, the NeuriteQuant freeware is the one that gives results more similar to control analysis and is more suitable to our raw microphotographs, acquired in real acquisition conditions that are hardly reproducible from literature to the real laboratory settings.

Chapter 4

Phase Contrast Images - Developing new tools

4.1 Software tools for phase contrast microscopy

The phase contrast optical imaging technique is used in brigthfield microscopy to enhance contrast of unlabelled and even unprocessed biological samples, such as live cells in culture.

In phase contrast microscopy, the contrast of the image is improved in two steps. The background light is phase shifted by passing through a phase shift ring. This eliminates the phase difference between the background and the scattered light, that leads to an increase in the intensity difference between the foreground and the background. To further increase the contrast, the background is dimmed by a gray filter ring. Some of the scattered light is also phase shifted and dimmed by the rings, but in a lesser extent[36].

Phase contrast images do not need antibodies or dyes and therefore can be inexpensive in terms of imaging reagents. Moreover, there is no need of spending time in antibodies incubation nor in any previous sample preparation, making this a potential good method of neuronal analysis. As staining is not usually used for these images, the cells remain alive after the analysis, another relevant characteristic of this imaging technique. Nonetheless, there are also disadvantages to this technique, which include: the difficulty to analyse these images due to their intrinsic low contrast, namely between the object of interest and the image background; uneven illumination that results from shinning a light on two-dimensional objects; and vignetting (darkening of the corners of the image with a spotlight appearance)[37].

Unexpectedly, there are few freeware tools capable of analysing phase contrast images of neurons and neuronal cultures in an automatic or semi-automatic manner.

4.1.1 NeuronGrowth

Our search for freeware tools was dedicated to automatic or semi-automatic analysis of neurons only retrieved NeuronGrowth. NeuronGrowth is a program for the automatic

quantification of extension and retraction of neurites and fillopodia from time-lapse sequences of two dimensional bioimages. NeuronGrowth was implemented in Java, as an independent and multi-platform system containing entire digital image processing modules. The program needs a previous semi-automatic characterization of neurites in a reference image, which is further used for the automatic tracking and measurement of neurites in the time sequence images. The program includes some preprocessing modules like sequence alignment, background subtraction, flat field correction, light normalization, and cropping. In phase contrast images this program can be used to track and measure neurites, and in fluorescence images it can be used to track fillopodia. This program was implemented as a free plug-in for ImageJ [38].

Unfortunately, this program can not be applied to our images since these are not obtained from time-lapse experiments where the same sample field is imaged through time. It would be therefore necessary to mark all the neurites manually if this program was to be used.

4.1.2 Image Processing techniques for phase contrast image analysis

Image Preprocessing

Before applying a program for the quantitative analysis of neuronal phase contrast images, as the image of Figure 4.1, in most of the cases preprocessing steps are needed to enhance contrast, remove dead cells, and correct the illumination. Some of the tools available in ImageJ dedicated to perform image preprocessing are described below.

- Contrast enhancement

In the ImageJ environment there are some tools designed to enhance contrast. The *Contrast Limited Adaptive Histogram Equalization (CLAHE)* plugin enhances the local contrast of an image, and is called through the menu *Process / Enhance Local Contrast (CLAHE).*

Contrast enhancement can also be achieved using mathematical morphology, by creating Top-hat and Bottom-hat processed images of the original one. The Top-hat image is used to highlight the brightest spots and extract the small elements in the input image, while the Bottom-hat image is used to emphasize the gaps between the objects of the original image. These tools can be used to enhance contrast by a method described by [32] and [34] that consists in adding the Top-hat image and subtracting the Bottom-hat image to the original, maximizing the contrast between the objects and the gaps that separate them. Figure 4.2 results from the application of this method to the original Figure 4.1, using ImageJ tools.

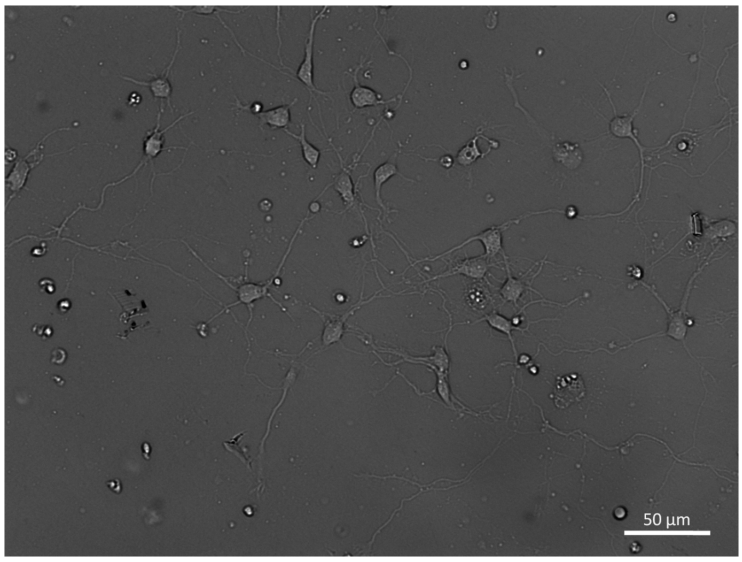

Figure 4.1: Example of an original phase contrast neuronal image to be digitally analysed. Microphotography obtained at 4 div.

- Debris removal

Thresholding the enhanced image will result in binary objects comprising not only living cells but also dead cells and noise components (see Chapter 2). Thus, it is necessary to remove these unwanted foreground components (dead cells and other debris) during that process. This can be achieved by setting criteria for unwanted image components based on a subset of features such as intensity and particle circularity, which have to be defined by the user. Particles to be removed have to fulfil all the criteria, which is set in an empirically manner by testing the parameters in components of the image that the user knows to be signal, such as live cells bodies.

In the case of Figure 4.2, the value of the threshold applied to it was 100 pixels, meaning that the particles in the image with a intensity value over 100 are selected for potential removal. The value of the particles' area size was set to 400 pixels and the circularity criteria was established between 0.3 and 1; this means that all the particles whose area is below 400 pixels and with circularity parameters inside that circularity interval are potential noise. Particles that have all these characteristics, and thus fulfil all the criteria, are considered dead cells or debris and are consequently removed. Figure 4.3 shows the result of the application of this method to Figure 4.2; note the removal of bright dead cells throughout the image.

- Illumination correction

In image recognition it is always assumed that the same type of feature has the same brightness wherever they appear in the field of view. This assumption is equivalent to stating that the illumination is uniform. One of the approaches to illumination correction

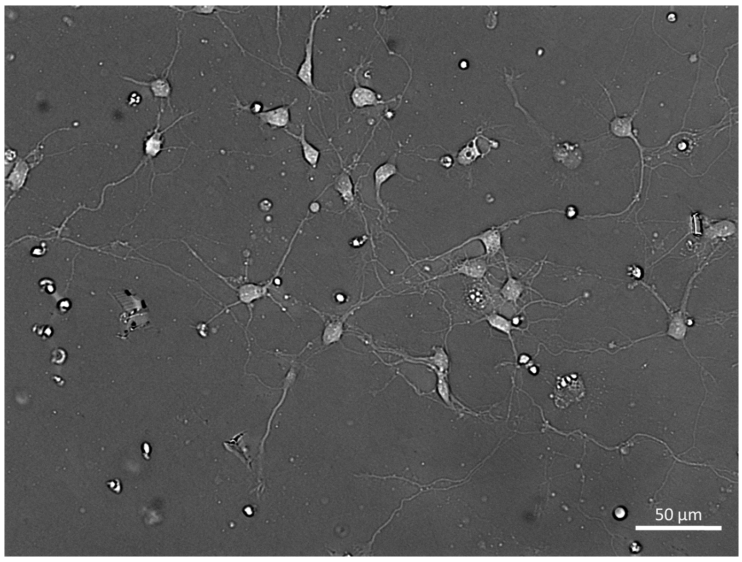

Figure 4.2: Image 4.1 with its contrast enhanced by using a circle with 20 pixels as a structural element.

can be based on a method similar to the proposed by Leong et al [35]. The idea is to estimate an approximation of the background intensity function. This is accomplished by computing a lowpass-filtered version of the image and subtracting it from the original. In order to obtain a reasonable approximation for the background behaviour, the filter is normally build upon a large Gaussian kernel with the standard deviation setted to be 120 pixels. Figure 4.4 shows the resulting image after illumination correction of Figure 4.3; the illumination was improved but the cell bodies appear fragmented and/or with holes.

Another method to correct uneven illumination is using the Top-hat transform[39]. In Figure 4.5 is used a Top-hat transform with a circle with 20 pixels as a structural element, applied to Figure 4.2. Here, the illumination was corrected and the soma and neurites are clearly visualized; some bright smaller dots appear that can be easily removed in posterior steps

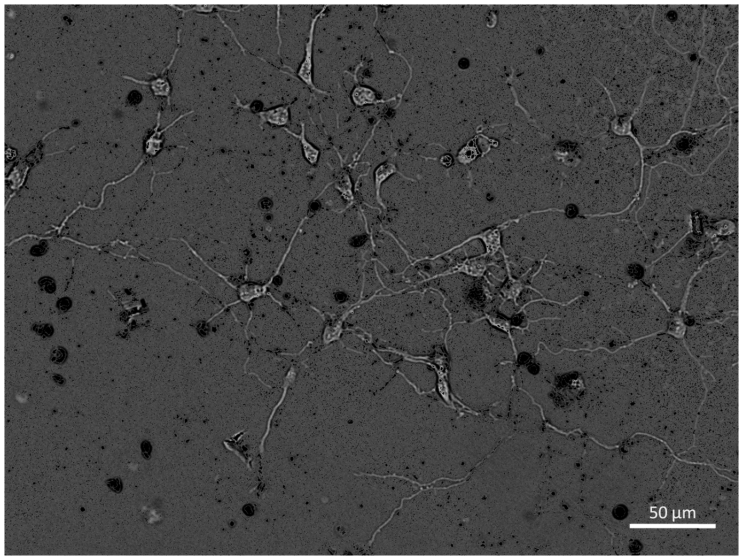

Figure 4.3: Image 4.1 after dead cells and debris removal by thresholding.

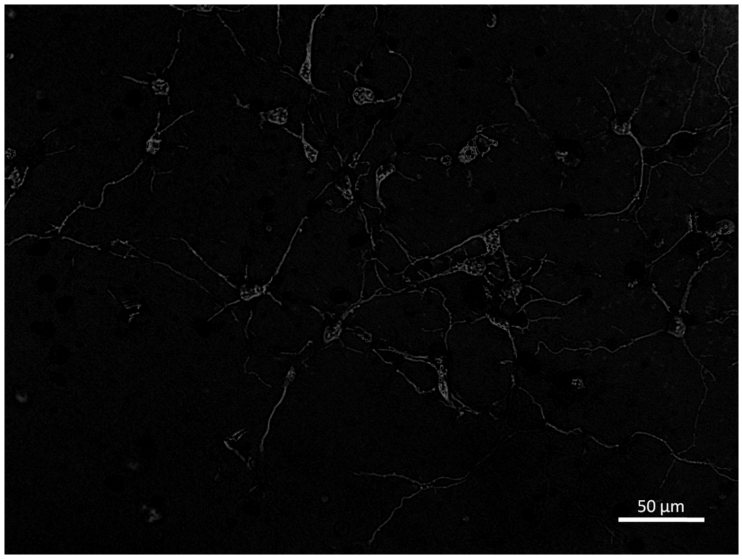

Figure 4.4: Image 4.3 after the illumination correction using a Gaussian blur of 120 pixels in Figure 4.3.

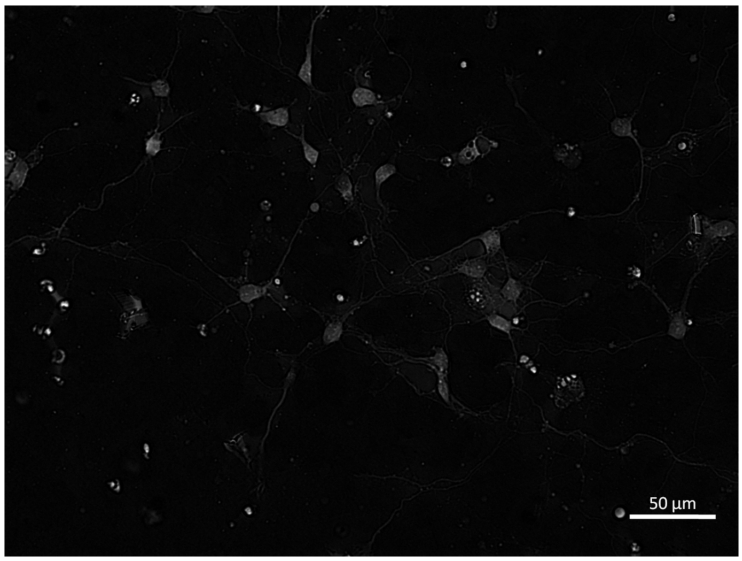

Figure 4.5: Image 4.2 after the illumination correction using the Top-hat transform. The image used to perform this operation was Figure 4.2.

Segmentation

Image segmentation provides a set of disjoint regions in the image according to some criteria and often involves *a priori* knowledge. The aim is that some of these regions will match our objects of interest [22].

- Cell bodies segmentation

Cell body segmentation is achieved by a morphological opening operation (an erosion followed by a dilation)[22]. This removes the thin neuritic mask and leaves the cell bodies.

- Neuritic Segmentation

To segment the neurites of an image it is necessary to subtract from it the previously obtained image with the mask of the cell bodies. To improve the process it is also necessary to reduce the noise and enhance the edges to better find the neurites; for this purpose we can use the Difference of Gaussians (DoG), which is a differential operator that provides a numerical estimate for the second derivative of the underlying image. The first Gaussian kernel is used to smooth the image and suppress high-frequency noise, while the second Gaussian kernel, with a larger standard deviation, removes both the noise and important edges, lines and details. The difference between the two images keeps only the structures that have an intermediate size range between the two operators.

A similar method to enhance edges under controlled noise levels is the *Laplacian of Gaussian* edge detector that first smooths the image with a Gaussian before performing the second derivative computation to enhance the edges.

Feature extraction

The next step after the segmentation is to measure the individual features of each object. The command `analyse skeleton` can be used to obtain the length of the neurite network, while the command `analyse particles` can be used in the mask of cell bodies to obtain the features of the cell bodies. The features quantified in the mask of cell bodies are the number of cells, the area - which is the pixel area of the interior of the object, and circularity - a parameter obtained using the formula $4\pi \times area/perimeter^2$ [20], with a value of 1.0 indicating a perfect circle.

By using these image processing techniques it is possible to design a macro script to run within the ImageJ environment that provides an efficient support for the semi-automated quantitative analysis of this peculiar kind of images. The commands workflow and their settings will be described in the next section.

4.2 NeuronNet macro for neuronal phase contrast bioimages

4.2.1 Preprocessing

Contrast enhancement

To perform contrast enhancement we used mathematical morphology by creating Top-hat and Bottom-hat processed images of the raw image. By adding the Top-hat image and subtracting the Bottom-hat image to the original image the contrast was enhanced. The structural element used to perform these operations was a circle with a radius of 20 pixels, and the original and enhanced images are the ones previously presented in Figure 4.1 and 4.2, respectively.

Illumination correction

In the NeuroNet macro we can skip the debris removal preprocessing step since we will use the Top-hat method to correct illumination and, with this method, the macro does not include debris as cell bodies (as it can be observed in the resulting image Figure 4.6), since debris are usually removed through a erosion and the cell bodies are selected by size. This Top-hat transform was setted with a 20 pixels circle as the structural element.

4.2.2 Segmentation

Cell body segmentation

To segment cell bodies we used the Top-hat image that we have previously obtained. To this Top-hat image (Figure 4.5) it is first applied an erosion with a structural element of 2 pixel, of radius, to separate the cells, and then an opening is applied with a structural element of 5, since it gave the best results upon an erosion of 2 pixels, in terms of cell body recognition and less false positives. Then, a threshold is applied to get the cell bodies and the command *analyse particles* is used to create a mask of these cell bodies. The result can be observed in Figure 4.6. This step may still require user interaction in order to fine tune the results - compare cell bodies segmentation of Figure 4.7, obtained after user interaction, with the ones of Figure 4.6 (obtained automatically).

Neuritic enhancement and segmentation

To segment the neurites we have first created a Top-hat image obtained with a structural element of 25 pixels applied to the previously contrast enhanced image, enhanced its contrast through CLAHE, and finally subtracted the image with the mask of cell bodies from this enhanced Top-hat image. Following, we have used the 'Difference of Gaussians' method to improve the process by reducing the noise and enhancing the edges of the neurites. The first Gaussian kernel smooths the image and was set to have 1 pixel of radius,

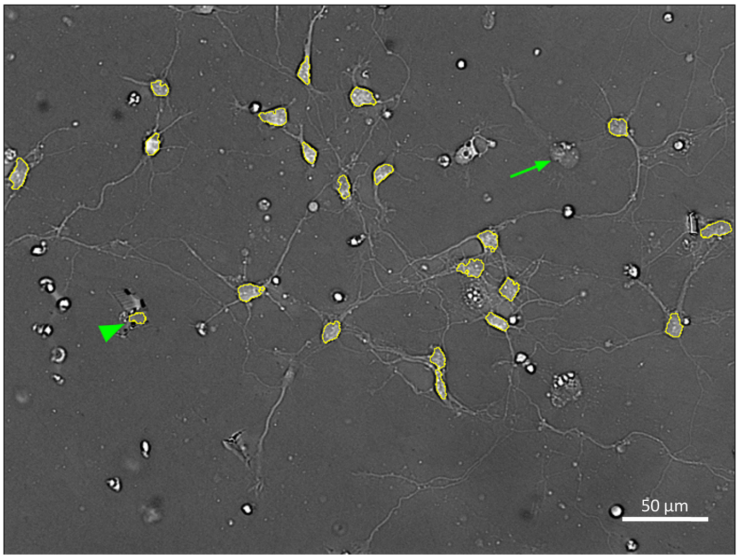

Figure 4.6: Image derived from Figure 4.5 image following the application of the automatic cell body segmentation processing; the cell bodies are marked without user interaction. Note that some cell bodies were not detected by the macro (false negatives, arrows), while others do not correspond to real cell bodies of live cells (false positives, arrowheads).

while the second Gaussian kernel that removes both the noise and important edges was set to 3 pixels. The difference between the two images (resulting from subtracting the image with a Gaussian blur of 3 from the image a Gaussian blur of 1) keeps only the structures that have an intermediate size range between the two operators.

The resulting image is binarized (transformed in 0/1 images, with background values set to 0 and foreground values set to 1) using a predefined threshold that varied accordingly to the developmental period of the cells (time in culture: intensity value of 5, 3 and 1 for 4, 10 and 14 div images, respectively). To remove the remaining noise that was still present in the image we used the command *analyse particles* to remove particles with a size smaller than 22, 17 or 10 pixels in 4, 10 and 14 div images, respectively. These values were empirically determined for each time period, being the ones that gave the best results in terms of debris removal. In Figure 4.8 it is possible to observe the binarized image of the neurites. Afterwards, a mask with particles with circularity over 0.8 was created, since the cell body are not present in this image and the neurites present circularity usually below 0.4. This mask was subtracted to image in Figure 4.8, in order to remove noise that was still present (see Figure 4.9).

With the binary image it is possible to use the command skeletonize to make skeletons of the neurites and measure their length, as demonstrated in Figure 4.10. This command iteratively erodes structures down to a thickness of 1 pixel without splitting them.

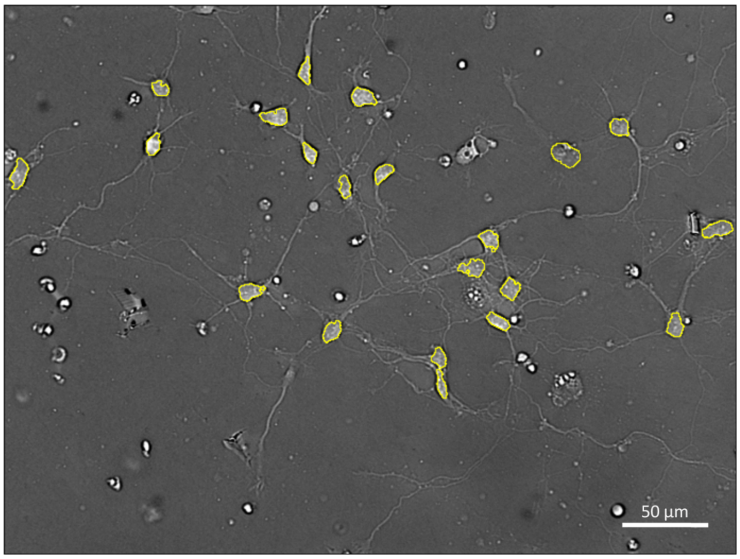

Figure 4.7: Image derived from Figure 4.5 following the application of cell body segmentation processing and user interaction; the cell bodies that were previously not marked by the macro (Figure 4.6) were manually depicted.

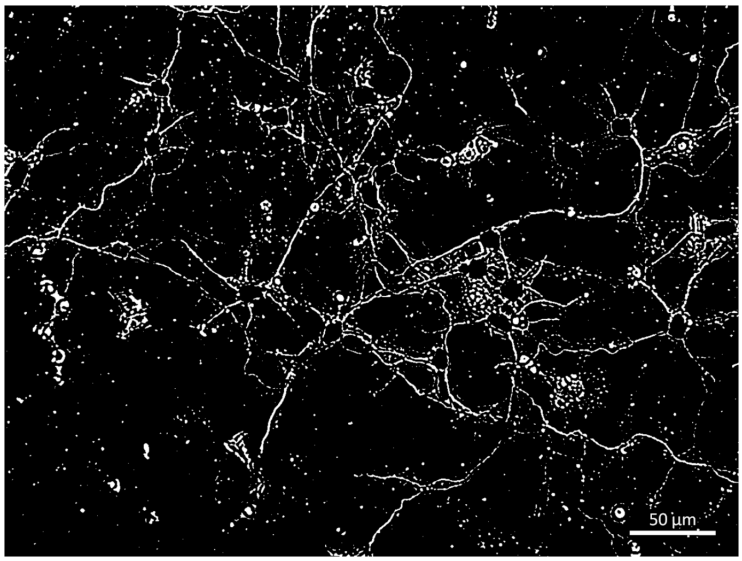

Figure 4.8: Image showing binarized segmented neurites (derived from Figure 4.5, upon subtraction of the cell body mask shown in yellow in Figure 4.7.

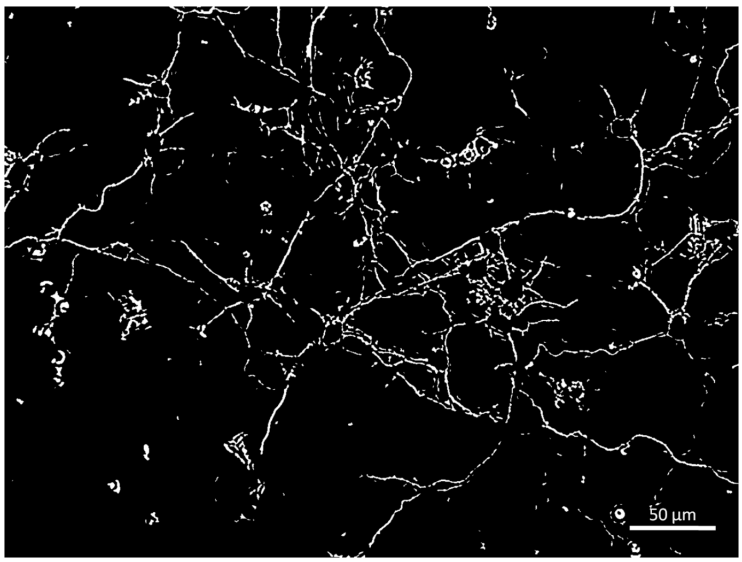

Figure 4.9: Image of binarized segmented neurites after the removal of particles with circularity over 0.8.

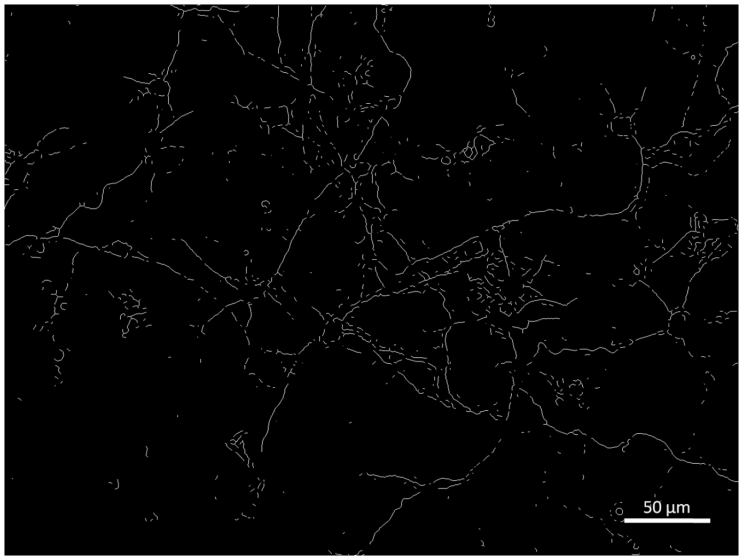

Figure 4.10: Image showing the skeleton of the neurites (derived from Figure 4.9).

4.2.3 Feature extraction

The final step of image processing is to measure the individual features of each object. We use the command *analyse skeleton* to obtain the neuritic network length of Figure 4.10, and the command *analyse particles* in the mask of cell bodies to quantify the number of cells, the area (in pixels), and circularity (with a value of 1.0 indicating a perfect circle). The total image area occupied by the neurons, expressed as percentage of the total area of the image, was measured in Figure 4.11, an image where neurites were added to the mask of cell bodies. Of note, to better analyse the efficiency of the NeuroNet macro, this 'end' image was always visually compared to the original raw image (here Figure 4.11 vs Figure 4.1)

In Figures 4.12 and 4.13 we can find the parameters usually obtained by the macro. In the image we have named "Mask" (cell bodies mask image) we have obtained the information about the number of cells, average size of each neuronal cell body and mean cell body circularity. From the image we have named "cell-body-neurites" we extracted the percentage of area occupied by the cell bodies plus the neuritic network, and from the image we have named "neurite" we extracted the information of the percentage of area occupied only by the neuritic network.

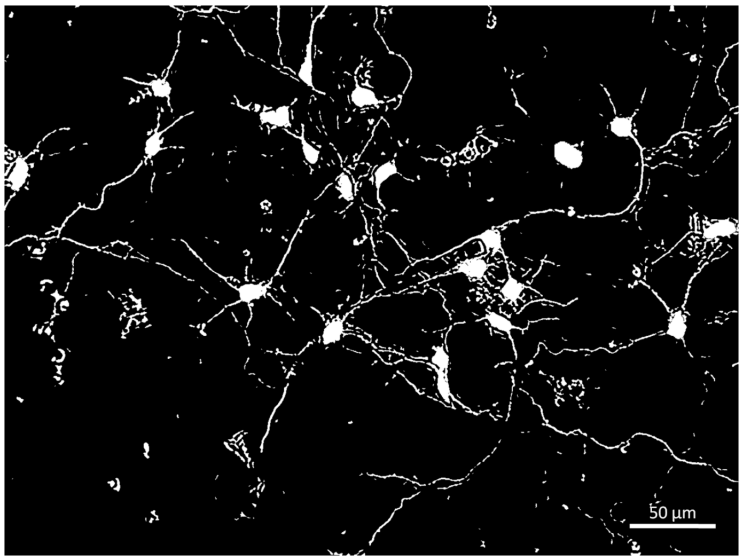

Figure 4.11: Image with the cell bodies added to the image of neurites.

Summary

File Edit Font

Slice	Count	Total Area	Average Size	%Area	Mean	Circ.	Solidity	IntDen
Mask	21	19213.000	914.905	1.353	255	0.629	0.889	233300.714
neurites	935	57911.000	61.937	4.078	255	0.514	0.690	15793.909
cell_bodies_neurites	828	80309.000	96.992	5.655	255	0.521	0.692	24732.844

Figure 4.12: Parameters obtained by the NeuroNet macro. The parameters underlined are the most relevant for comparing phase contrast images of neuronal cultures in different conditions (see Chapter 5). Values are given in pixels.

Branch information

File Edit Font

	Skeleton ID	Branch length	V1 x	V1 y	V1 z	V2 x	V2 y	V2 z	Euclidean distance
1098	917.000	8.243	1348.000	221.000	0.000	1355.000	218.000	0.000	7.616
1099	918.000	24.899	1350.000	577.000	0.000	1372.000	574.000	0.000	22.204
1100	919.000	6.828	1351.000	589.000	0.000	1357.000	587.000	0.000	6.325
1101	920.000	2.828	1352.000	270.000	0.000	1354.000	268.000	0.000	2.828
1102	921.000	4.828	1356.000	182.000	0.000	1358.000	186.000	0.000	4.472
1103	922.000	5.828	1356.000	266.000	0.000	1358.000	261.000	0.000	5.385
1104	923.000	9.071	1356.000	449.000	0.000	1362.000	455.000	0.000	8.485
1105	924.000	5.414	1356.000	908.000	0.000	1361.000	909.000	0.000	5.099
1106	925.000	5.828	1358.000	258.000	0.000	1360.000	253.000	0.000	5.385
1107	926.000	1.000	1358.000	433.000	0.000	1358.000	434.000	0.000	1.000

Figure 4.13: Window with the neuritic skeleton analysis. The values of the column "Branch length" are subsequently summed in the program MS Office Excel to obtain the Total Neuritic Length. Values are given in pixels.

Chapter 5

Phase contrast images - a case study

The NeuroNet macro developed in Chapter 4 to tackle specific image processing problems of neuronal cultures of phase contrast images was applied to various sets of images from two different experimental conditions - Control and N-[N-(3,5- difluorophenacetyl)-l-alanyl]-S-phenylglycine t-butyl ester (DAPT), a pharmacological inhibitor - at three different culture incubation periods: 4, 10 and 14 div, in order to extract quantitative data from these and to test the macro.

5.1 Control condition

The macro NeuroNet was first applied to the three sets of phase contrast microscopy images (4, 10 and 14 div) taken under basal control conditions. Results are provided in the following Tables (5.1 to 5.3). All the images analysed in this chapter were obtained with a 20× objective in an epifluorescence inverted Olympus IX microscope. Each of the images has the size of 1376 × 1032 pixels, which in micrometers corresponds to 444 × 333 micrometers.

4 div images

In 4 div images (Table 5.1) the average Number of Cells per image is 30.4 ± 3.3 cells, with the minimum value per image being 11 cells (image 3) and maximum value being 43 cells (image 4), with this creating a great range for this parameter (a SEM that represents 11% of its mean) (Figure 5.10). The Cell Body Area has a mean of 132.3 ± 2.8 μm^2, with an amplitude of 29.2 μm^2 (Figure 5.4). The Circularity has a low range of values, with a mean of 0.80 and an amplitude of 0.05.

The Total Network Length tends to change with the number of cells in the image, with its highest value (10960.6 μm) being in the image with the highest number of cells, image 4, as expected. The Neurite Length per Cell (8346.5 ± 747.7 μm) has a great variability due to the non homogeneity of the network along the culture: an amplitude about 95% of its mean, and a SEM that represents 10% of its mean, similar to the SEM of Total Neurite Length that is around 9% of its mean. This possibly indicates the need to analyse

Table 5.1: Primary and secondary parameters retrieved by the NeuroNet macro in the analysis of phase contrast microscopy images of neuronal primary cultures at 4 div. Description of each parameter can be found in Chapter 2.

Image	Number of cells	Cell body area	Circularity per cell	% of Total Area Occupied by the Neurites	% of Total Area Occupied by the Neurites plus the cell bodies	Total neurite length	Neurite length per cell
1	20	129.0	0.79	3.2	5.0	4253.5	212.7
2	30	138.0	0.77	6.1	9.1	7669.7	255.7
3	11	142.3	0.81	4.3	5.5	5413.9	492.2
4	43	113.1	0.81	9.0	12.3	10960.6	254.9
5	26	129.8	0.82	6.3	8.7	8789.7	338.1
6	41	127.1	0.82	8.5	12.3	10627.7	259.2
7	39	135.7	0.80	7.3	10.8	9349.4	239.7
8	27	137.7	0.81	7.9	10.7	9398.7	348.1
9	37	137.5	0.82	6.5	10.2	8654.8	233.9
Mean	30.4	132.3	0.80	6.6	9.4	8346.5	292.7
SEM	3.3	2.8	0.01	0.6	0.8	747.7	29.2

a larger number of images due to the non homogeneity of the network along the culture. The area occupied by the neuronal culture (Figure 5.6) has a mean of $9.4 \pm 0.8\%$. This mainly reflects the contribution from the neuritic network, whose area represents 70% of the total area occupied by the culture. In Figure 5.1 is presented a example image of this condition.

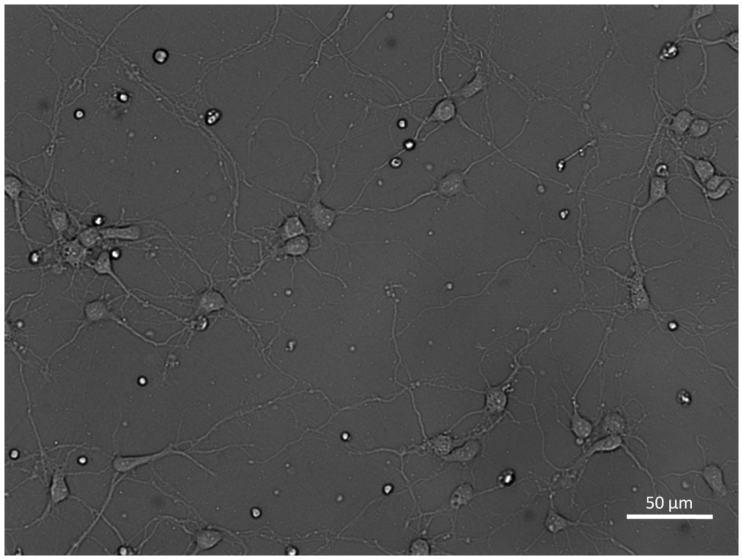

(a) image a.

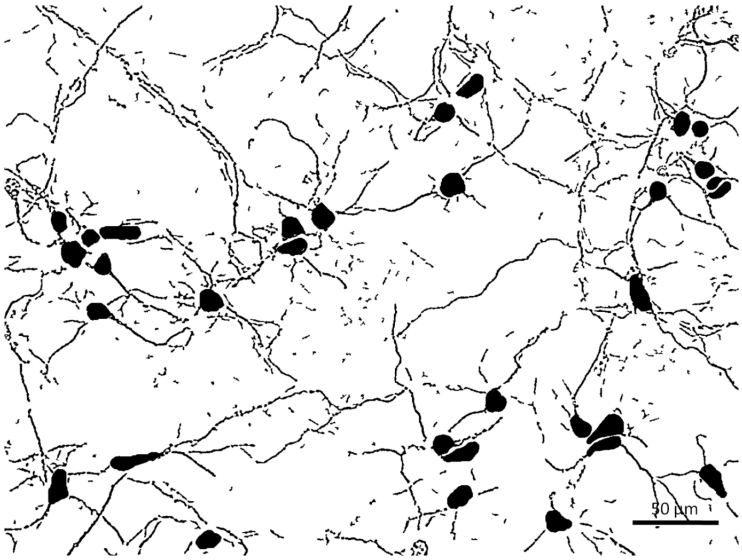

(b) image b.

Figure 5.1: Original phase contrast image of 4 div control group (a) analysed with the NeuroNet macro (b).

Table 5.2: Primary and secondary parameters retrieved by the NeuroNet macro in the analysis of phase contrast microscopy images of neuronal primary cultures at 10 div. Description of each parameter can be found in Chapter 2.

Image	Number of cells	Cell body area	Circularity per cell	% of Total Area Occupied by the Neurites	% of Total Area Occupied by the Neurites plus the cell bodies	Total neurite length	Neurite length per cell
1	34	151.4	0.81	22.2	26.0	27819.7	818.2
2	25	180.5	0.81	23.5	26.6	27232.3	1089.3
3	33	143.3	0.82	19.7	22.9	22528.4	682.7
4	25	156.5	0.82	13.6	16.5	16316.5	652.7
5	26	173.9	0.85	19.8	23.0	22691.3	872.7
6	19	147.0	0.82	17.0	19.1	20925.2	1101.3
7	33	158.1	0.82	20.3	24.4	21746.1	659.0
8	27	163.0	0.83	19.3	22.5	23601.9	874.1
9	39	143.3	0.80	17.5	21.8	19938.4	511.2
Mean	29.0	157.4	0.82	19.2	22.5	22533.3	806.8
SEM	2.0	4.4	0.01	1.0	1.1	1109.9	63.2

10 div images

In 10 div control images (Table 5.2) a smaller amplitude is evident in the Number of Cells per image, while the mean (29 cells) remains constant (when compared to 4 div images), as expected since neurons do not perform mitosis. The range of values for the Cell Area is higher due to the influence of image 2, with a value of 180.5, that is far from the mean (157.4 ± 4.4 μm^2, Table 5.2), with its mean being significantly different from 4 div images (Figure 5.4). The Circularity keeps the range of 0.05 and is therefore the most stable parameter, not changing with time in culture (Figure 5.5). Of note, the circularity parameter has a SEM that represents only 1% of its mean, while the Cell Area SEM is around 3%, and the Cell Number has a SEM of 7% of its mean.

Regarding Total Network Length (22533.3 μm), image 4 shows the lowest value (16316.5 μm), even though it does not present the lowest number of cells. This can be due to an error in the segmentation of the neurites by the program, resulting in a great range of values for this parameter. The Neurite Length per Neuron (806.8 μm) has a great amplitude since images 2 and 6 have twice the value of the Neurite Length per Neuron of image 9. This parameter has a SEM of 8%, while the Total Neurite Length SEM represents only 5% of its mean. As expected, these parameters regarding the neuritic network increased with time in culture, including the Area occupied by neuronal soma and neurites (Figure 5.6). The area occupied by the neuronal culture has a mean of 22.5 ± 1.1%, with an increased contribution from the neuritic network since it now represents 85% of the total neuronal area (Figure 5.6). In Figure 5.2 a image of this group condition is analysed with the NeuroNet macro.

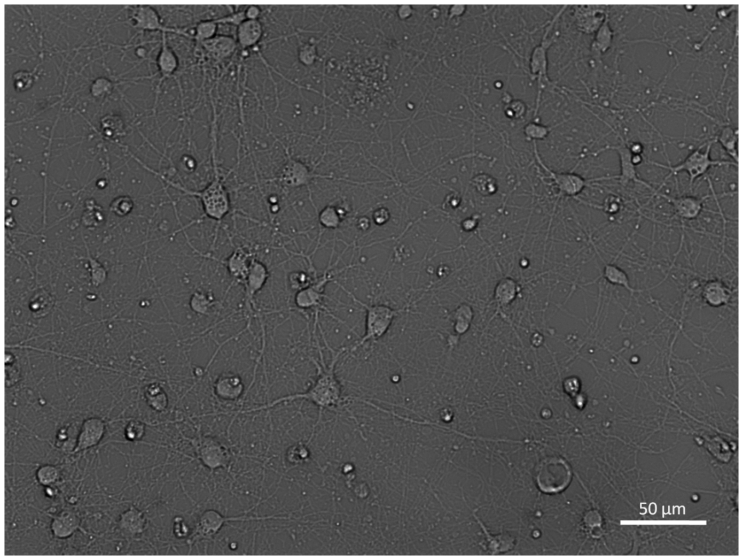

(a) image a.

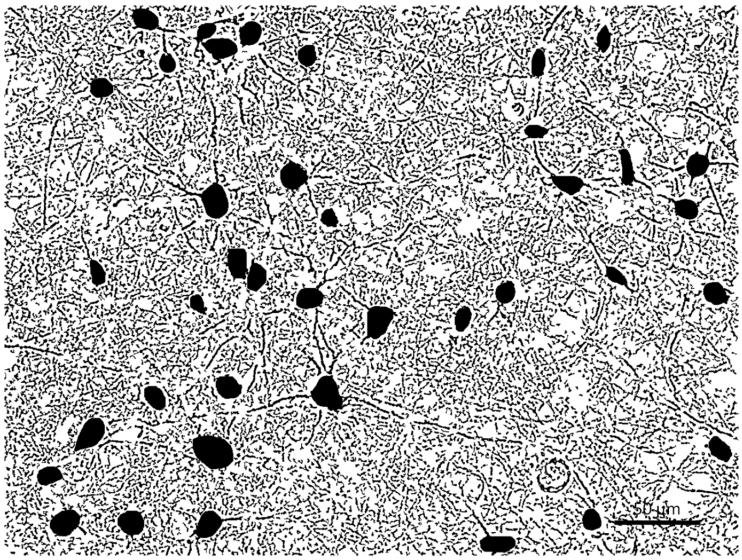

(b) image b.

Figure 5.2: Original phase contrast image of 10 div control group (a) analysed with the NeuroNet macro (b).

Table 5.3: Primary and secondary parameters retrieved by the NeuroNet macro in the analysis of phase contrast microscopy images of neuronal primary cultures at 14 div. Description of each parameter can be found in Chapter 2.

Image	Number of cells	Cell body area	Circularity per cell	% of Total Area Occupied by the Neurites	% of Total Area Occupied by the Neurites plus the cell bodies	Total neurite length	Neurite length per cell
1	43	137.3	0.82	38.8	44.0	48060.6	1117.7
2	35	134.2	0.79	40.6	43.9	48462.3	1384.6
3	41	125.8	0.82	38.1	41.8	41621.6	1015.2
4	27	116.0	0.80	37.3	39.6	41017.4	1519.2
5	61	151.5	0.80	39.4	46.0	41899.7	686.9
6	38	140.0	0.81	39.7	43.8	48688.7	1281.3
7	35	137.9	0.83	40.1	43.4	48551.6	1387.2
8	37	149.4	0.84	39.9	43.6	49339.0	1333.5
9	36	147.7	0.82	39.7	43.7	46691.0	1297.0
10	27	143.0	0.82	39.1	41.7	46802.6	1733.4
11	31	159.9	0.82	40.0	44.0	49128.4	1584.8
12	42	138.7	0.81	39.0	43.1	46137.4	1098.5
13	59	135.4	0.82	38.5	44.1	48411.6	820.5
14	22	182.4	0.82	40.3	43.0	47684.8	2167.5
15	63	125.6	0.80	37.4	43.1	45369.4	720.1
Mean	39.8	141.6	0.81	39.2	43.3	46524.4	1276.5
SEM	3.2	4.1	0.00	0.3	0.4	729.8	101.8

14 div images

In 14 div images there is a higher Number of Cells than in 4 and 10 div images (39.80 ± 3.2) and this parameter also presents a high amplitude, reflected in its SEM (8% of the mean) (Table 5.3). These values were not expected and can be due to the fact that the images analysed were acquired in high density cell clusters or/and to the presence of some glia cells in the culture. In general the Cell Body Area is constant (SEM of 2.9% of the mean) with the exception of image 14, with a value of 182 μm^2 and is similar to 4 div images (Figure 5.4). The Circularity remains similar and is still the parameter that presents less variability (Figure 5.5).

The Total Neurite Length (46524.4 ± 729.8 μm) is almost constant at this period (SEM around 2% of the mean), more constant than in 10 div images, which may reflect structural maturation of the network. The Neurite Length per cell has a mean of 1276.5 ± 101.8 μm and has a great variability (SEM around 8% of the mean) due to the variation in the number of cells from image to image. The area occupied by the neuronal culture presents a mean value of $43.3 \pm 0.4\%$. The contribution from the neuritic network has a higher value than in 4 and 10 div images, as expected, and represents now 91% of the total area occupied by the culture (Figure 5.6). Figure 5.3 is a representative image of this group.

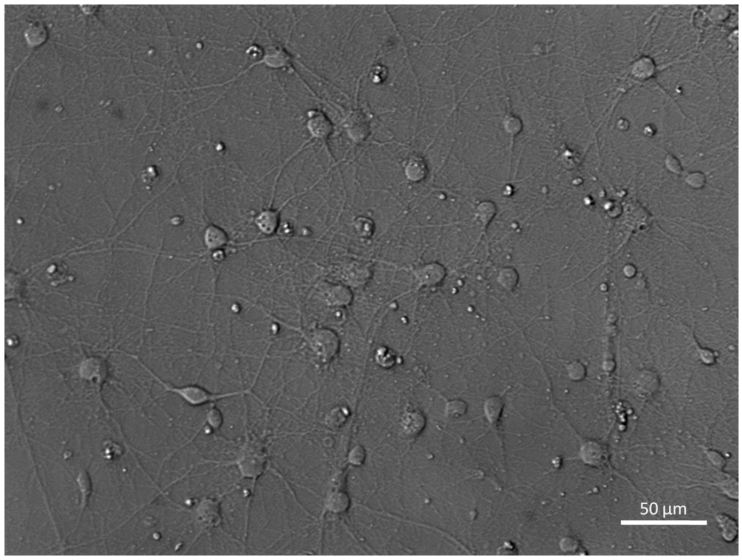

(a) image a.

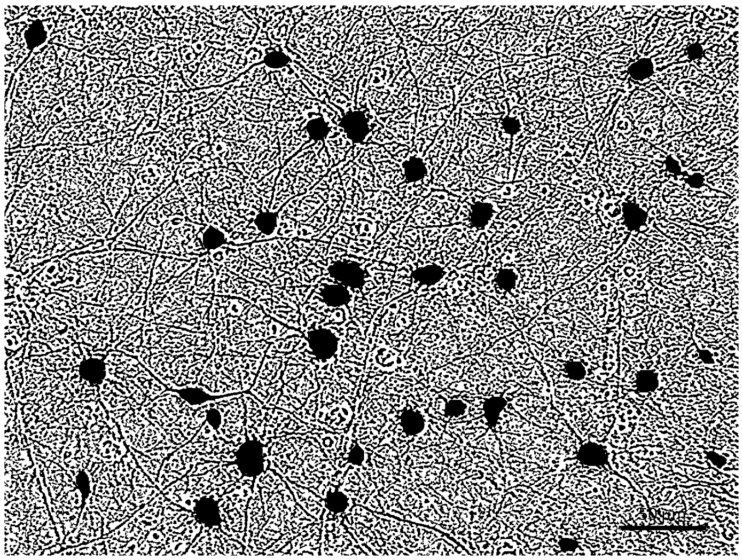

(b) image b.

Figure 5.3: Original phase contrast image of 14 div control group (a) analysed with the NeuroNet macro (b).

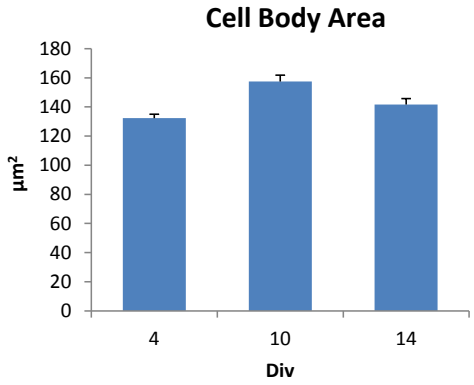

Figure 5.4: Graphic with the Cell Body Area of phase contrast microscopy images of neuronal primary cultures at 4, 10 and 14 div in control conditions. Data were tested with the Kolmogorov and Smirmov method to test for normality and all groups passed. The sample were also tested to observe if the standard deviation is identical using the method of Barlett, which suggested that the difference among the SD was not significant. Using the Tukey-Kramer Multiple Comparisons Test to analyse the significance of values the following results were obtained: $p<0.01$ for 4 vs 10; $p>0.05$ (ns) for 4 vs 14; $p<0.05$ for 10 vs 14 div.

In terms of the variation of these neuronal parameters with time in culture, it is possible to observe in Figure 5.4 that the Cell Body Area values are statistically different between 4 vs 10 div and 10 vs 14 div images, what was not expected. In Figure 5.5 it is possible to observe as expected the data from Cell Body Circularity do not present any statistically significant differences between any values, as expected. Furthermore, with time in culture, both the values for Neuritic and Neuronal Area present significantly differences between 4, 10 and 14 div images (Figure 5.6), as expected for a developing culture. The percentage of contribution of the neurites to the neuronal network increases with time from 70% at 4 div to 85% at 10 div and 91% at 14 div, as expected.

5.2 DAPT conditions

DAPT is a pharmacological drug that inhibits the cleavage of a transmembranar protein, the Alzheimer's Amyloid Precursor Protein (APP), which is involved in cell adhesion and neuritogenesis, with APP being required for synaptogenesis, synapse remodeling and neurite outgrowth in neurons.[40] [41]. In other cell lines this drug has been observed to increase the number of preneuritic processes (our unpublished results) and thus its potential effects in the establishment of the neuritic network in cortical primary neuronal cultures were assessed here.

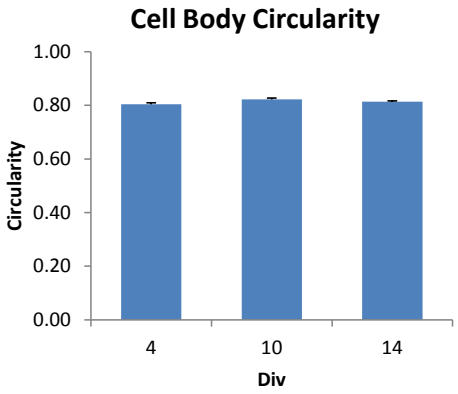

Figure 5.5: Graphic with the circularity of phase contrast microscopy images of neuronal primary cultures at 4, 10 and 14 div in control conditions. The 10 div and 14 div group did not pass the Kolmogorov and Smirnov Test for normality, and hence we used the Kruskal-Wallis test to analyse the variation among column medians, with the values not being significantly greater than expected by chance.

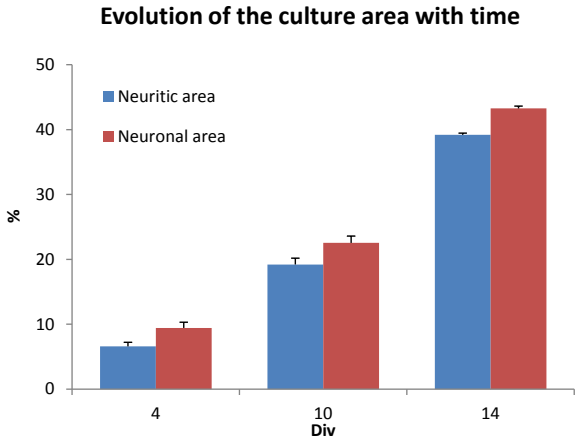

Figure 5.6: Graphic with the neuritic and neuronal area of phase contrast microscopy images of neuronal primary cultures at 4, 10 and 14 div in control conditions. The 4, 10 and 14 div groups passed in the Kolmogorov and Smirnov Test for normality of neuritic area, however the method of Barlett suggests that the differences among the Standard Deviation is significant; due to this, non parametric tests were used to compare the results. Using the Welch corrected Unpaired t test to analyse the significance of values, the following results for neuritic area were obtained: $p<0.0001$ for 4 vs 10; $p<0.0001$ for 4 vs 14; $p<0.001$ for 10 vs 14 div. The neuronal area group 14 div did not pass in the normality test, so in the statistical analysis non parametric tests were also used. Using the Welch corrected Unpaired t test, to analyse the significance of values the following results for neuronal area were obtained: $p<0.001$ for 4 vs 10; $p<0.0001$ for 4 vs 14; $p<0.0001$ for 10 vs 14 div.

Table 5.4: Primary and secondary parameters retrieved by the NeuroNet macro in the analysis of phase contrast microscopy images of neuronal primary cultures at 4 div after 24h incubation with 1 μmol DAPT. Description of each parameter can be found in Chapter 2.

Image	Number of cells	Cell body area	Circularity per cell	% of Total Area Occupied by the Neurites	% of Total Area Occupied by the Neurites plus the cell bodies	Total neurite length	Neurite length per cell
1	30	124.2	0.76	7.3	10.1	9513.9	317.1
2	39	124.4	0.84	8.7	12.0	11373.5	291.6
3	42	115.3	0.82	7.0	10.7	9415.8	224.2
4	38	128.2	0.83	8.1	11.7	9942.3	261.6
5	35	131.4	0.81	9.1	12.6	11710.3	334.6
6	33	118.2	0.83	7.2	10.0	9815.8	297.4
7	26	136.7	0.77	6.8	9.4	9065.8	348.7
8	33	110.9	0.77	6.0	8.7	7925.5	240.2
9	39	121.0	0.79	8.2	11.3	10467.4	268.4
10	46	117.3	0.80	7.9	11.6	10158.1	220.8
11	54	121.9	0.81	8.8	13.5	11639.7	215.5
12	34	137.9	0.83	6.7	10.1	7925.8	233.1
Mean	37.4	123.9	0.80	7.7	11.0	9912.8	271.1
SEM	2.2	2.4	0.01	0.3	0.4	366.7	13.4

4 div images

The 4 div DAPT images exhibit a higher Number of Cells per image (Table 5.4) than the 4 div control images, with a mean of 37.4 ± 2.2 (SEM of 6% of the mean) vs 30.4 ± 3.3 cells in control (Figure 5.10). The Area of the Cell Bodies does not change substantially and has a mean of 123.9 ± 2.4 μm^2 with a SEM of 2% vs 132.3 ± 2.8 μm^2 in control cells (Figure 5.11). The mean Circularity per cell is 0.80 ± 0.01 with a SEM below 1%, still being the most constant value.

Total Neurite length has a mean value of 9912.8 ± 366.7 μm (SEM of 3.7% of mean), with this value being higher than in control images (8346.5 ± 747.7 μm), but not statistically significant. In contrast, the Network Length per cell mean was very similar: 271.1 ± 13.4 μm (SEM around 5%) vs 292.7 ± 29.7 μm in control (Figure 5.13). This may result from the slightly higher number of cells in DAPT conditions (Figure 5.10). This fact can also explain the following: the area occupied by the neuronal culture is slightly higher than in control conditions (11.0 ± 0.4% vs 9.4 ± 0.8% in control); but the neuritic network, however, has a contribution to this value of 70% in both samples (Figure 5.12). In Figure 5.7 is presented a representative image of this group.

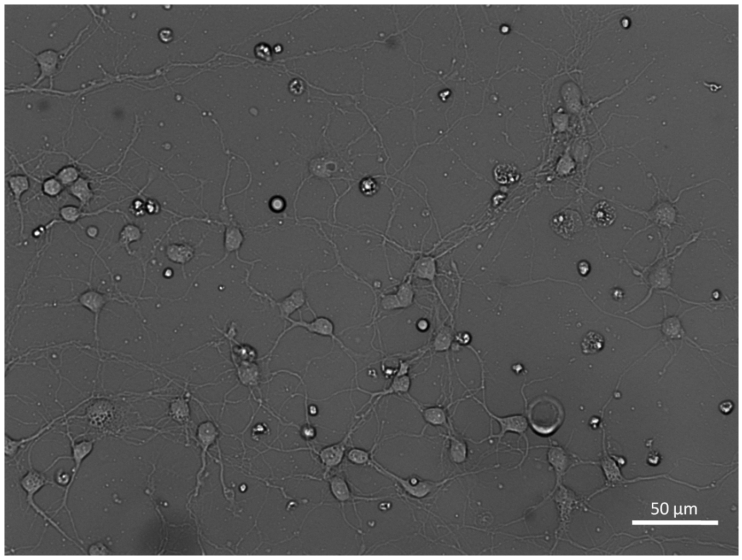

(a) image a.

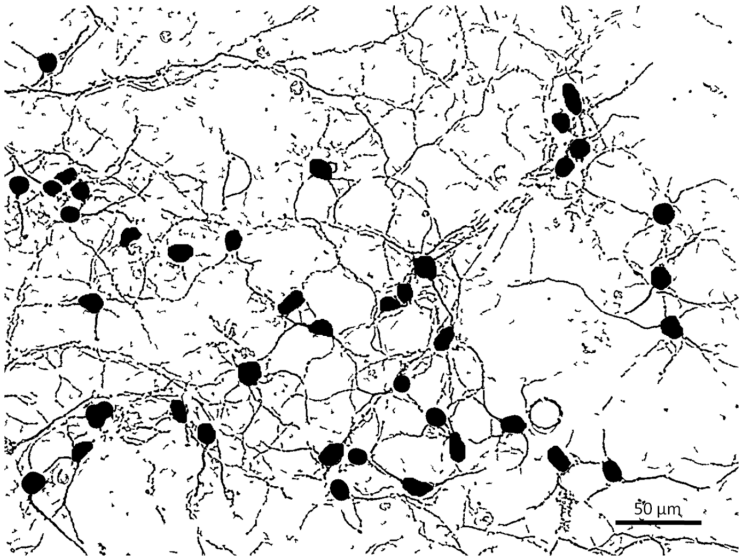

(b) image b.

Figure 5.7: Original phase contrast image of 4 div DAPT group (a) analysed with the NeuroNet macro (b).

Table 5.5: Primary and secondary parameters retrieved by the NeuroNet macro in the analysis of phase contrast microscopy images of neuronal primary cultures at 10 div after 24h incubation with 1 μmol DAPT. Description of each parameter can be found in Chapter 2.

Image	Number of cells	Cell body area	Circularity per cell	% of Total Area Occupied by the Neurites	% of Total Area Occupied by the Neurites plus the cell bodies	Total neurite length	Neurite length per cell
1	21	173.3	0.80	21.6	24.4	26034.5	1239.7
2	31	176.0	0.84	21.6	25.2	23556.8	759.9
3	20	144.0	0.82	16.7	18.8	20551.0	1027.5
4	18	203.0	0.82	23.2	25.9	28876.5	1604.2
5	18	201.2	0.84	29.0	31.5	36382.9	2021.3
6	31	161.2	0.84	20.2	24.2	23763.5	766.6
7	29	159.6	0.81	18.4	21.8	21738.4	749.6
8	24	153.0	0.84	17.5	20.0	21135.5	880.6
9	34	137.8	0.81	13.8	17.2	15260.3	448.8
10	10	166.7	0.84	16.5	17.6	19542.9	1954.3
11	20	156.2	0.82	21.1	23.2	25447.4	1272.4
Mean	23.3	166.5	0.82	20.0	22.7	23844.5	1156.8
SEM	2.2	6.3	0.00	1.2	1.3	1664.6	155.9

10 div images

There was a considerable decrease in the Number of Cells (23.3 $\pm$2.2 cells) relatively to 4 div images (37.4 $\pm$2.2 cells) and also to 10 div control conditions (29.0 $\pm$2.1 cells), leading us to suspect that between the 4 and 10 div time periods some cells died, or that these images were taken in lower density areas of culture. The Cell Body Area remains constant (166,5 $\pm$6.3 μm^2), SEM of 3.8% relatively to control conditions (157,4 $\pm$4.4 μm^2) (Figure 5.11). The Circularity (0.82 $\pm$0.00) remains constant in relation to control condition and 4 div DAPT images. Total Neurite Length has a mean of 23844.5 $\pm$1644.6 μm (similar to control conditions, 22533.3 $\pm$1109.9 μm). Two images contribute to this slightly high amplitude: image 9 has a value below the mean, albeit it is the image with more cells; possibly, due to the characteristics inherent to the image such as the presence of cell clusters, the readings have been affected. On the other hand, image 5, with a lower cell count than image 9, presents a total neurite length greater than the mean value. In agreement, the Area occupied by the Neuronal culture is equal in both conditions (22.7 $\pm$ 1.3% for DAPT vs 22.5 $\pm$ 1.1% in control), and mainly reflects the contribution from the Neuritic Network, whose area represents 88% of the total area occupied by the culture (85% in control group) (Figure 5.12). The Neurite Length per Cell is of 1156.8 $\pm$155.9 μm, presenting a huge variability, with a minimum of 448.8 μm and a maximum of 2021.3 μm. Interestingly, the mean Network Length per Cell value is higher than in 10 div control images (806.8 $\pm$63.2 μm) and close to the value of 14 div control images (1276.5 $\pm$101.8 μm) (Figure 5.13). This appears to result from the lower Number of Cells for this condition and time point. In Figure 5.8 is presented a representative image of this group.

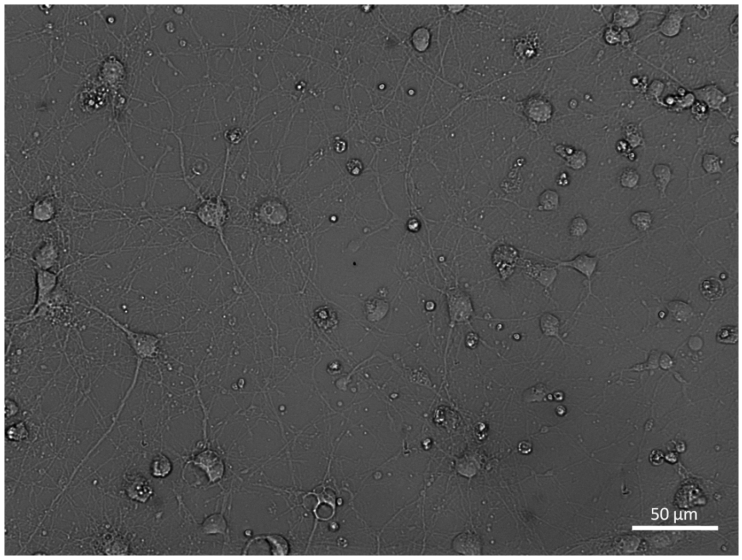

(a) image a.

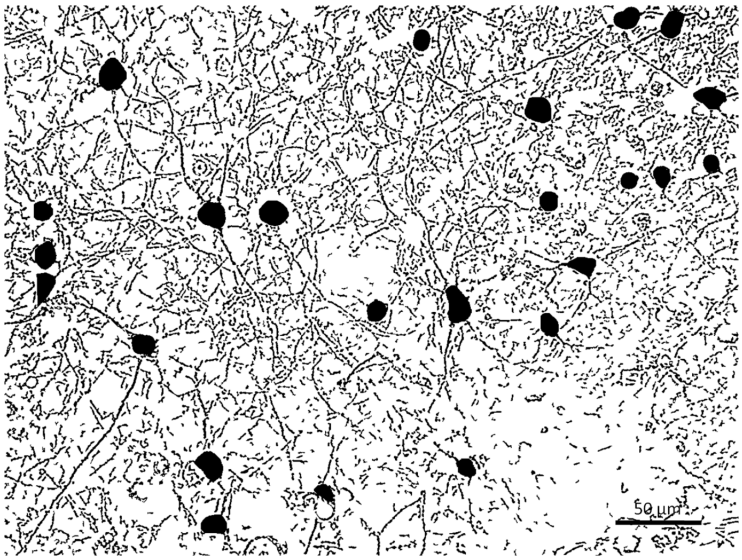

(b) image b.

Figure 5.8: Original phase contrast image of 10 div DAPT group (a) analysed with the NeuroNet macro (b).

Table 5.6: Primary and secondary parameters retrieved by the NeuroNet macro in the analysis of phase contrast microscopy images of neuronal primary cultures at 14 div after 24h incubation with 1 μmol DAPT. Description of each parameter can be found in Chapter 2.

Image	Number of cells	Cell body area	Circularity per cell	% of Total Area Occupied by the Neurites	% of Total Area Occupied by the Neurites plus the cell bodies	Total neurite length	Neurite length per cell
1	19	196.9	0.77	38.3	40.8	46099.0	2426.3
2	29	189.5	0.77	39.0	42.7	44761.3	1543.5
3	25	165.6	0.84	39.8	42.7	47848.4	1913.9
4	36	149.3	0.83	39.9	43.5	43677.7	1213.3
5	24	254.3	0.78	39.3	43.8	44835.2	1868.1
6	49	144.3	0.82	38.9	43.6	48976.8	999.5
7	26	167.9	0.83	39.9	43.0	47080.3	1810.8
8	35	152.9	0.84	39.4	43.0	45025.5	1286.4
9	37	148.1	0.83	39.8	43.7	43675.2	1180.4
10	30	147.3	0.84	38.9	42.4	46332.9	1544.4
11	40	166.2	0.84	40.4	45.2	47649.7	1191.2
12	47	134.5	0.82	40.3	44.8	49238.7	1047.6
13	52	128.6	0.84	40.0	45.1	47656.8	916.5
14	37	142.2	0.83	39.6	45.0	48977.4	1323.7
Mean	34.7	163.4	0.82	40.6	44.2	46559.6	1447.6
SEM	2.7	8.7	0.01	0.2	0.3	517.0	114.3

14 div images

The mean Number of Cells per image in the 14 div DAPT images (Table 5.6) is 34.7 $\pm$2.7, similar to control group (39.8 ± 3.2) and to 4 div DAPT images (37.4 ± 2.2), but higher than in 10 div DAPT images (23.3 ± 2.2); this indicates that 10 div images were not representative of the general cellular population. The Cell Body Area has a mean of 163.4 $\pm$8.7 μm^2 that is higher than in control group, 141.7 $\pm$4.1 μm^2, but the difference was not statistically significant (Figure 5.11). The mean Circularity per cell (0.82 ± 0.01) almost did not change between control and DAPT conditions or with time in culture, remaining as the most constant parameter.

Total Neurite Length was constant among the sample, with a mean value of 46559.6 $\pm$517.0 μm, and is very similar to the mean of the control group: 46559.6 $\pm$517.0 μm. The Neurite Length per Cell has a high variability in between the sample images (amplitude of 1510 μm), with a mean of 1447.6 $\pm$114.3 μm (SEM of 8%), similar to the control group, 1276.5 $\pm$101.8 μm (Figure 5.13). The Area occupied by the Neuronal culture has a mean of 44.2 $\pm$0.3%, similar to the control group (43.3 ± 0.4%) (Figure 5.12) and, as in control, the major contribution to Neuronal culture results from the Neuritic Network, whose area represents 92% of the total area occupied by the culture (91% in control group). In Figure 5.9 is presented a representative image of this group.

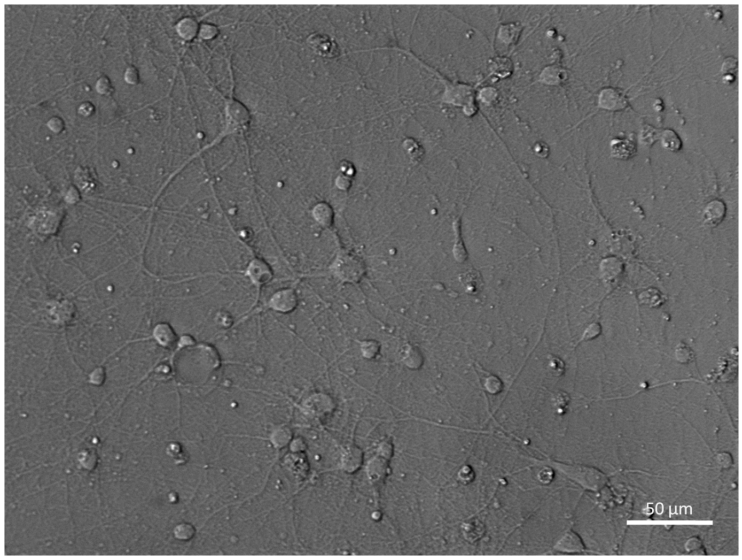

(a) image a.

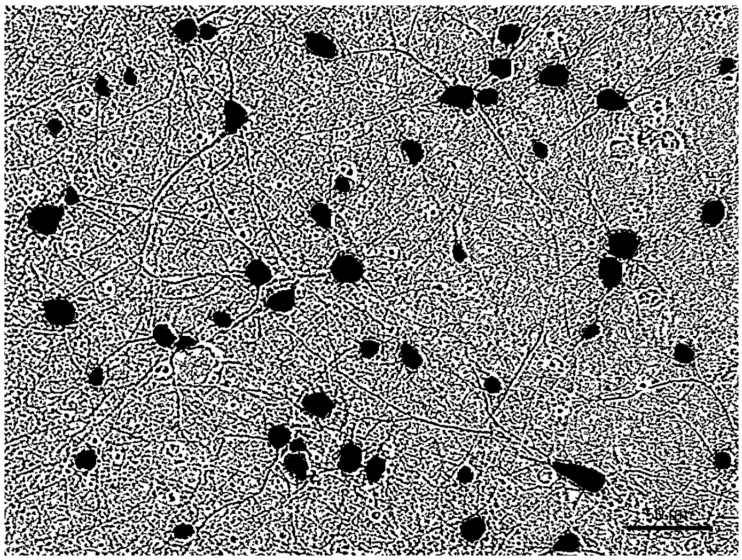

(b) image b.

Figure 5.9: Original phase contrast image of 14 div DAPT group(a) analysed with the NeuroNet macro (b).

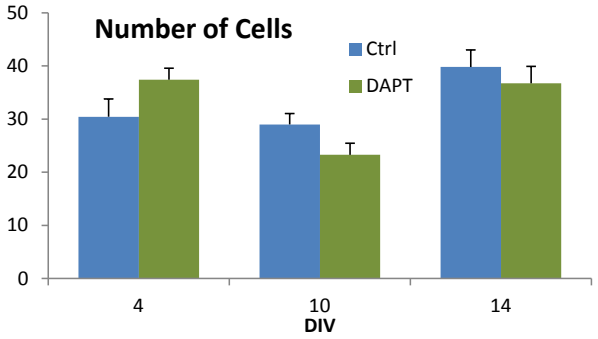

Figure 5.10: Graphic presenting the Number of Cells of phase contrast microphotographs of 4, 10 and 14 div neuronal primary cultures, in both control and DAPT conditions. All the groups passed in the Kolmogorov and Smirnov test for normality and Bartlett's test suggests that the differences among the standard deviation are not significant. Using the Unpaired t test to compare the values of 4 div control vs 4 div DAPT (p=0.0933), 10 div control vs 10 div DAPT (p=0.0766) and 14 div control vs 14 div DAPT (p=0.2363) we have concluded that these were not statistically different.

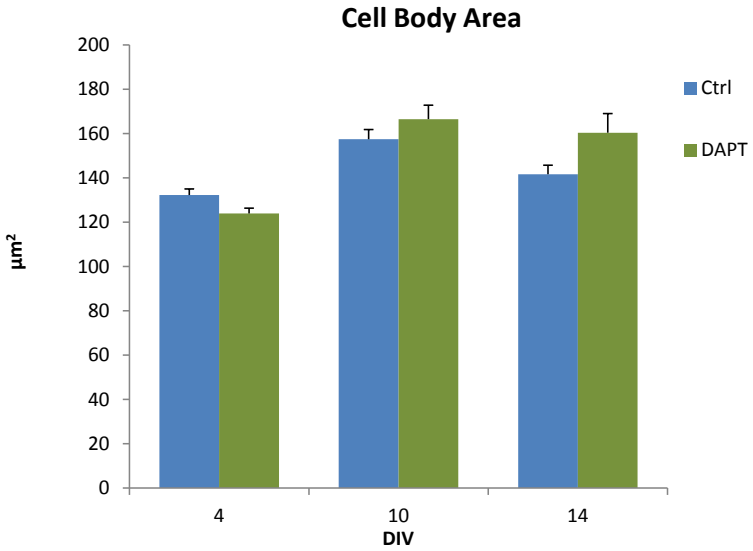

Figure 5.11: Graphic presenting the Cell Body Area of phase contrast microphotographs of 4, 10 and 14 div neuronal primary cultures, in both control and DAPT conditions. One of the groups did not pass in the Kolmogorov and Smirnov test for normality. So the samples were tested using non-parametric methods. Using the Mann-Whitney test to compare the values 4 div control vs 4 div DAPT (pv=0.04), 10 div control vs 10 div DAPT (pv=0.3232), 14 div control vs 14 div DAPT (pv=0.0196).

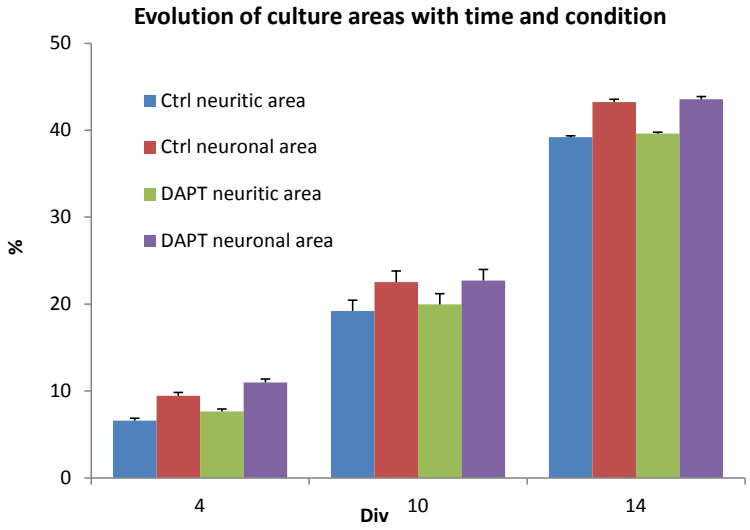

Figure 5.12: Graphic with the Neuritic and Neuronal areas of phase contrast microphotographs of 4, 10 and 14 div neuronal primary cultures, in both control and DAPT conditions. One of the groups did not pass in the Kolmogorov and Smirnov test for normality. So the samples were tested using non-parametric methods. Using the Mann-Whitney test to compare Neuritic Area values of 4 div control vs 4 div DAPT (p=0.3216), 10 div control vs 10 div DAPT (p=0.6200), 14 div control vs 14 div DAPT (p=0.6620); Neuronal Area of 4 div control vs 4 div DAPT (p=0.2551), 10 div control vs 10 div DAPT (p>0.9999), 14 div control vs 14 div DAPT (p>0.9999). All the results were not statistically different.

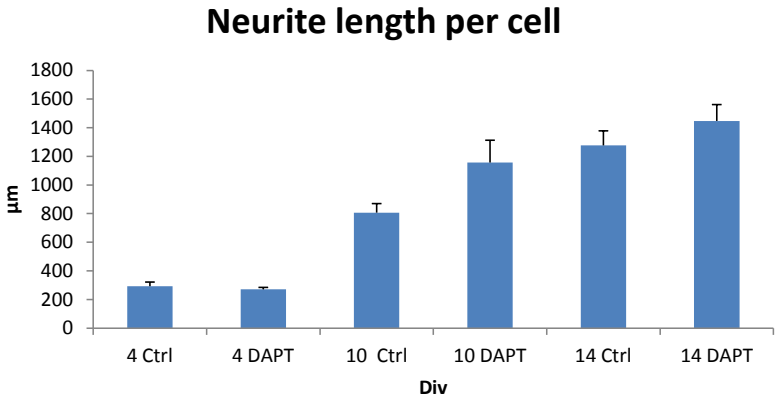

Figure 5.13: Graphic with the Neurite Length per Cell of phase contrast microphotographs of 4, 10 and 14 div neuronal primary cultures, in both control and DAPT conditions. One of the groups did not pass in the Kolmogorov and Smirnov test for normality. So the samples were tested using non-parametric methods. Using the Mann-Whitney test to compare the Neurite Length per Cell of 4 div control vs 4 div DAPT (pv=0.7664), 10 div control vs 10 div DAPT (pv<0.0001), 14 div control vs 14 div DAPT (pv>0.4253).

Chapter 6

Discussion and Conclusion

6.1 Fluorescence images

In what concerns fluorescence images of neuronal cultures, in the major part of the parameters evaluated, all programs retrieved results not statistically different from the ones resulting from the manual analysis taken as control. Specifically, for the Cell Body Area present results not statistically different from manual analysis taken as control; however, the programs that present closer cell body area results are NeuriteQuant and NeurphologyJ in raw images, since both the programs present higher results with preprocessed images. The mean Neurite Length per Cell is the parameter that presents more variability among the programs. The programs that present values closer to the manual analysis are NeuronJ with a coefficient of determination(r^2) of 0.993, followed by NeuriteQuant (r^2=0.926) with raw images, and NeurphologyJ (r^2=0.631) in preprocessed images (Figure 6.1). The program NeuriteQuant with raw images has a mean value closer to the one resulting from manual analysis but presented a larger SEM than NeuronJ, and the manual analysis. These two are very similar, as expected, since NeuronJ has a high contribution from the user. Concerning Attachment Points, both NeuriteQuant and NeurphologyJ (with preprocessed images) present values higher than the manual analysis, but with raw images the values obtained were lower than control. The program NeuriteQuant with preprocessed images present not quite significant differences, and NeurphologyJ/ri presented statistically different results from control, being the two pairs program/type of images more dissimilar than manual analysis. In relation to the detection of the Ending Points, all the programs present results much higher than the ones from manual analysis, being therefore all statistically different. This is possibly due to the high fragmentation of the neurites mainly by the programs in the segmentation step. Nonetheless, again the pair NeuriteQuant, raw images was the one closer to control analysis. For the determination of Neurite Branching, all the programs also present values higher than manual analysis, due to the great overestimation of the Ending Points and since the branching value is calculated by the ration between the number of Ending Points and the number of Attachment Points. Noteworthy, since the manual analysis was done by only one operator, it is not possible to observe the variability

inter-operators and possible errors deriving from subjective analysis.

From all the previous analysis the program that seems to work better with our 4 div fluorescence images is NeuriteQuant, applied to raw images, since it is automatic and gives overall results more similar to the manual analysis; this is particularly true for the evaluation of the Neurite Length per cell (Figure 3.2). One of the drawbacks is that the quantification of neuritic ramification is better to be performed manually, since although the number of Attachment Points are close to the manual analysis, the same does not occur with the Ending Points (Figure 3.4). NeuriteQuant can automatically evaluate/extract more morphological parameters than the other freeware (see Table 2.2), and future mark will include to test its ability to quantify neuronal parameters not presented here due to limitations of the other freeware.

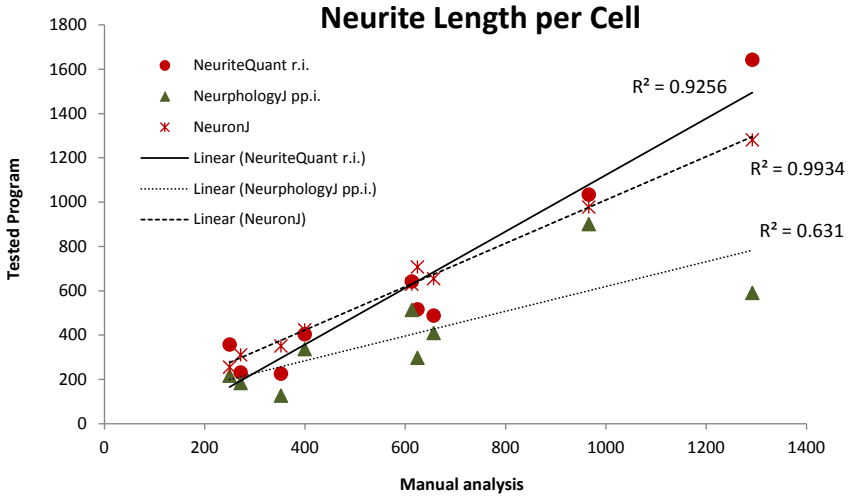

Figure 6.1: Correlation of the parameter Neurite Length per Cell by the programs NeuronJ, NeuriteQuant/r.i. and NeurphologyJ/pp.i. with the manual analysis.

6.2 Phase contrast images

Phase contrast images are easy to obtain, are almost cost-free, and may not imply killing the cells in the sample. In the other hand, these images present a very low signal-to-noise ratio and may have uneven illumination.

Few or none freeware could be found to analyse this type of images, leading us to develop a new macro, named NeuroNet since it is aimed to evaluate the status of neuronal networks at different conditions (time, pharmacologically, etc).

First, this macro was applied to microphotographs of cultures in control conditions at a different time points of development (4, 10 and 14 div). The results obtained were as expected, with an increasing in neuritic length, both total and per cell, and also in the occupation area by the neuronal culture. Nonetheless, results for the 14 div images in comparison to 10 div - double values for the Neuritic Area (figure 5.3) and 1.5 fold increase in the Neuritic Length per Cell (Figure 5.7) were somewhat unexpected, since the culture should be morphologically mature around the 10 div period [9].

Further, the NeuroNet macro was applied to images of cultures at the same time periods but incubated with a drug that inhibits the cleavage of an adhesion protein, the APP. This drug was observed to increase the number of preneurites and neurites in immortalized cell lines (our data not published).

In 4 div images there is no statistical difference in the mean Number of Cells per image between DAPT and control group, although the DAPT group has slightly more cells. About the Cell Body Area there is a statistical significant difference between conditions, with the control group having higher Cell Body Area. In what concerns Neuritic and Neuronal Area, and Neurite Length per Cell, no statistical significant difference was found between the two conditions (Figure 5.6 and 5.7). This can be visualized in Figure 6.3, where the values extracted for each image Total Neurite Length are presented. Noteworthy, when using the NeuroNet macro in 4 div phase contrast images, taken in parallel to the fluorescence microphotographs of Chapter 3, the mean Neurite Length per Cell extracted is about one third of the value of the fluorescence images analysed manually. This huge difference can be due to the fact that GFP cDNA is better transfected into more mature cell, with higher neuritic length. In Figure 6.2 it is possible to compare a image of a neuron acquired with fluorescence microscopy with an image of the same neuron and non-fluorescing neighbours, acquired with phase contrast microscopy.

In 10 div images, the control group has more cells potentially indicating higher survival of the post-mitotic neurons, however the difference is not statistically significant. The Cell Body, Neuritic and Neuronal Area are almost identical between the control and DAPT groups. The only difference found is in the Neurite Length per Cell (Figure 5.7) in which the DAPT group has a value higher than in 10 div control group, and is more similar to 14 div control group. With this number of samples these differences were not statistically significant, and a higher n has to be used to assure their similarity, difference. The same is applied to the difference found in cell body area between control and DAPT conditions at 4 div.

In 14 div images the control group has more cells than the DAPT group but, as in 10

div images, this difference was not statistically significant. The Cell Body Area is higher in the DAPT group and as also observed in the 4 and 10 div images, the Number of Cells and the Cell Body Area appears to have an inverse relationship. This may be due to the presence of mitotic glial cells, which has to be further evaluated. The Neuritic and Neuronal Area are almost equal between the groups, suggesting that between 10 and 14 div may occur the maturation of the neuritic network.

In general, there are no differences in the control and DAPT conditions. We would like to also compare the number of attachment and ending points, and calculate the neurite branching, however, due to the characteristics of these phase contrast images (high ramification and number of neuritic contacts and crossovers/low signal to noise ratio), the neurites appear fragemented and therefore all these parameters would be overestimated. Overall, the increase in the percentage of area occupied by the neuronal culture and the neuritic network gives us strong indications of the macro capabilities. In regarding the effects of DAPT in the culture development, we would like to analyse the growth of neurons with the NeuroNet macro and with NeuronGrowth program at early development stages.

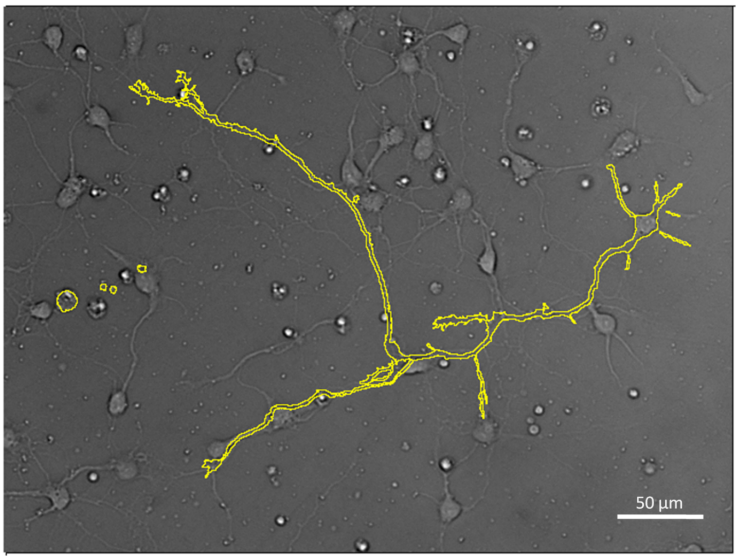

(a) Phase contrast image with the marked region of interest of a neuron acquired through fluorescence microscopy (the same of Figure 2.2).

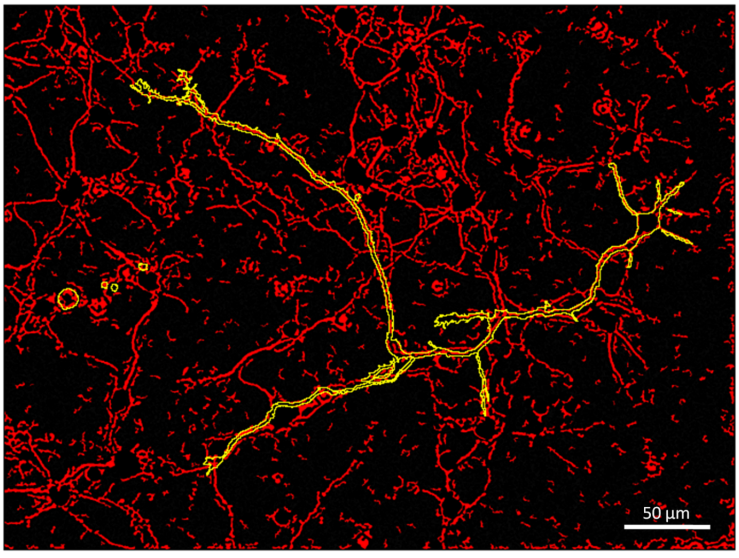

(b) Previous image following binarization with the result of segmentation of neurites with the NeuroNet macro.

Figure 6.2: Comparison of phase contrast with fluorescence microscopy.

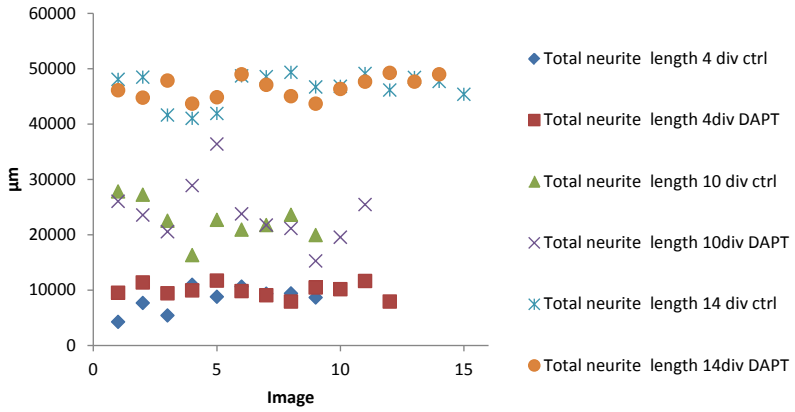

Figure 6.3: Values of Total Neurite Length for each image in 4, 10 and 14 div in both control and DAPT conditions.

6.3 Conclusion

The first objective of this thesis, which was to perform a function survey of the available tools for neuronal image processing, and its sub-objective of testing if the programs available better performed with a preprocessing step before the analysis, were accomplished. We thus propose the application of NeuriteQuant to raw fluorescent images with the caution that measurements of Attachment and Ending points should be performed manually for better results.

The second objective, of creating a workflow to extract relevant information of neuronal phase contrast images, was also accomplished with the development of the NeuroNet macro, which was further tested in our phase contrast images at different conditions with apparent success. We are still comparing the values obtained with ones reported in the literature, but few data/articles were found until now with morphometric data from rat cortical primary cultures. Of note, the NeuroNet macro has been already improved in the step of neuronal cell bodies segmentation.

Future work could include an increase in the number of samples(n) and testing more conditions in order to achieve better preprocessing settings in fluorescent microphotographs; include more observers for the manual analysis; survey digital solutions for neuritic fragmentation in programs such as Neurolucida. About the NeuroNet macro we aim to develop other methods to improve the removal of debris before the neurite segmentation, and to automate the process of extracting the total neurite length without needing to sum the values obtained with the skeletonization of neurites in the MS Office Excel.

Bibliography

[1] G. Xiong, X. Zhou, A. Degterev, L. Ji, and S. T. Wong, "Automated neurite labeling and analysis in fluorescence microscopy images," *Cytometry A*, vol. 69, no. 6, pp. 494–505, 2006.

[2] G. a. Ascoli, "Neuroinformatics grand challenges.," *Neuroinformatics*, vol. 6, pp. 1–3, Jan. 2008.

[3] E. Meijering, "Neuron tracing in perspective.," *Cytometry. Part A : the journal of the International Society for Analytical Cytology*, vol. 77, pp. 693–704, July 2010.

[4] R. R. Seeley, P. Tate, and T. D. Stephens, *Anatomy & physiology*. Dubuque, IA: McGraw-Hill, 8th ed., 2008.

[5] D. Purves, *Neuroscience*. Sunderland, Mass.: Sinauer, 4th ed., 2008.

[6] L. C. Kapitein and C. C. Hoogenraad, "Which way to go? Cytoskeletal organization and polarized transport in neurons," *Mol Cell Neurosci*, vol. 46, no. 1, pp. 9–20, 2011.

[7] M. M. Rolls, D. Satoh, P. J. Clyne, A. L. Henner, T. Uemura, and C. Q. Doe, "Polarity and intracellular compartmentalization of Drosophila neurons," *Neural Dev*, vol. 2, p. 7, 2007.

[8] M. Stiess and F. Bradke, "Neuronal polarization: The cytoskeleton leads the way," *Dev Neurobiol*, 2010.

[9] G. Dotti, A. Sullivan, C. Biology, A. M. College, and N. York, "The Establishment of Polarity by Hippocampal," no. April, 1988.

[10] J. Eberwine, K. Miyashiro, J. E. Kacharmina, and C. Job, "Local translation of classes of mRNAs that are targeted to neuronal dendrites.," *Proceedings of the National Academy of Sciences of the United States of America*, vol. 98, pp. 7080–5, June 2001.

[11] F. Costa, E. Tadeu, M. Manoel, F. Faucereau, J. Chelly, J. V. Pelt, and G. Ramakers, "A shape analysis framework for neuromorphometry," *Network: Computation in Neural Systems*, vol. 13, pp. 283–310, 2002.

[12] S. Y. Ho, C. Y. Chao, H. L. Huang, T. W. Chiu, P. Charoenkwan, and E. Hwang, "NeurphologyJ: an automatic neuronal morphology quantification method and its application in pharmacological discovery," *BMC Bioinformatics*, vol. 12, p. 230, 2011.

[13] J. Biranowska, J. Dziewiatkowski, B. Ludkiewicz, and J. Morys, "Developmental changes of synaptic proteins expression within the hippocampal formation of the rat," *Anat Embryol (Berl)*, vol. 206, no. 1-2, pp. 85–96, 2002.

[14] A. Lajtha, *Handbook of neurochemistry and molecular neurobiology. Neuronal signaling mechanisms* . New York: Springer, 3rd ed., 2009.

[15] M. Carter and J. C. Shieh, *Guide to research techniques in neuroscience*. Amsterdam ; Boston: Elsevier/Academic Press, 2010.

[16] M. D. Abràmoff, "Image processing with imageJ," *Biophotonics International*, 2004.

[17] M. M, B. A, and F. G., "Quantitative morphology and shape classification of neurons by computerized image analysis," *Computer Methods and Programs in Biomedicine*, vol. 41, 1993.

[18] D. E. Donohue and G. a. Ascoli, "Automated reconstruction of neuronal morphology: an overview.," *Brain research reviews*, vol. 67, pp. 94–102, June 2011.

[19] L. Dehmelt, G. Poplawski, E. Hwang, and S. Halpain, "NeuriteQuant: an open source toolkit for high content screens of neuronal Morphogenesis," *BMC Neurosci*, vol. 12, p. 100, 2011.

[20] T. Ferreira and W. Rasband, *ImageJ User Guide*. 2011.

[21] S. Chris and B. Toby, *Fundamentals of Digital Image Processing: A Practical Approach with Examples in MATLAB*. 2011.

[22] G. A. Baxes, *Digital image processing: principles and applications*. John Wiley & Sons, 1994.

[23] W. Burger and M. J. Burge, *Digital Image Processing: An Algorithmic Introduction Using Java*. Springer, 2008.

[24] A. Laurent, *Understanding Open Source and Free Software Licensing*. O'Reilly Media, 2004.

[25] G. Landy and A. Mastrobattist, *The IT / Digital Legal Companion: A Comprehensive Business Guide to Software, IT, Internet, Media and IP Law*. Syngress, 1 edition ed., 2008.

[26] M. Berg, C. Otfried, K. Marc, and O. Mark, *Computational Geometry Algorithms and Applications*. Springer, edition, t ed., 2008.

[27] M. L. Narro, F. Yang, R. Kraft, C. Wenk, A. Efrat, and L. L. Restifo, "NeuronMetrics: software for semi-automated processing of cultured neuron images.," *Brain research*, vol. 1138, pp. 57–75, Mar. 2007.

[28] M. Pool, J. Thiemann, A. Bar-Or, and A. E. Fournier, "NeuriteTracer: a novel ImageJ plugin for automated quantification of neurite outgrowth," *J Neurosci Methods*, vol. 168, no. 1, pp. 134–139, 2008.

[29] E. Meijering, M. Jacob, J. C. Sarria, P. Steiner, H. Hirling, and M. Unser, "Design and validation of a tool for neurite tracing and analysis in fluorescence microscopy images," *Cytometry A*, vol. 58, no. 2, pp. 167–176, 2004.

[30] Lyshevski Sergey E., *Engineering and Scientific Computations Using MATLAB*. Wiley-Interscience, 1 edition ed., 2003.

[31] W. Yu, H. K. Lee, S. Hariharan, W. Bu, and S. Ahmed, "Quantitative neurite outgrowth measurement based on image segmentation with topological dependence," *Cytometry A*, vol. 75, no. 4, pp. 289–297, 2009.

[32] Y. Zhang, X. Zhou, A. Degterev, M. Lipinski, D. Adjeroh, J. Yuan, and S. T. Wong, "A novel tracing algorithm for high throughput imaging Screening of neuron-based assays," *J Neurosci Methods*, vol. 160, no. 1, pp. 149–162, 2007.

[33] Y. Zhang, X. Zhou, A. Degterev, M. Lipinski, D. Adjeroh, J. Yuan, and S. T. Wong, "Automated neurite extraction using dynamic programming for high-throughput screening of neuron-based assays," *Neuroimage*, vol. 35, no. 4, pp. 1502–1515, 2007.

[34] D. N. Ponraj and M. E. Jenifer, "Morphological Operations for the Mammogram Image to Increase the Contrast for the Efficient Detection of Breast Cancer," *European Journal of Scientific Research*, vol. 68, no. 4, pp. 494–505, 2012.

[35] F. J. W.-M. Leong, M. Brady, and J. O. McGee, "Correction of uneven illumination (vignetting) in digital microscopy images.," *Journal of clinical pathology*, vol. 56, pp. 619–21, Aug. 2003.

[36] N. Shaked, *Biomedical Optical Phase Microscopy and Nanoscopy*. Academic Press, 2012.

[37] J. Sedgewick, *Scientific Imaging With Photoshop: Methods, Measurement, and Output*. New Riders, 1 edition ed., 2008.

[38] Z. Fanti, M. E. Martinez-Perez, and F. F. De-Miguel, "NeuronGrowth, a software for automatic quantification of neurite and filopodial dynamics from time-lapse sequences of digital images.," *Developmental neurobiology*, vol. 71, pp. 870–81, Oct. 2011.

[39] E. Dougherty and R. Lotufo, *Hands-On Morphological Image Processing*. 2003.

[40] T. Bittner, M. Fuhrmann, S. Burgold, C. K. E. Jung, C. Volbracht, H. Steiner, G. Mitteregger, H. a. Kretzschmar, C. Haass, and J. Herms, "Gamma-secretase inhibition reduces spine density in vivo via an amyloid precursor protein-dependent pathway.," *The Journal of neuroscience : the official journal of the Society for Neuroscience*, vol. 29, pp. 10405–9, Aug. 2009.

[41] U. C. Müller and H. Zheng, "Physiological Functions of APP Family Proteins.," *Cold Spring Harbor perspectives in medicine*, vol. 2, p. a006288, Feb. 2012.